Three-nucleon force in relativistic three-nucleon Faddeev calculations

H. Witała, J. Golak, R. Skibiński, W. Glöckle, H. Kamada, and W. N. Polyzou

Phys. Rev. C **83**, 044001 — Published 5 April 2011

DOI: 10.1103/PhysRevC.83.044001

Three-nucleon force in relativistic three-nucleon Faddeev calculations

H. Witała, J. Golak, and R. Skibiński

M. Smoluchowski Institute of Physics,

Jagiellonian University, PL-30059 Kraków, Poland

W. Glöckle

Institut für theoretische Physik II, Ruhr-Universität Bochum, D-44780 Bochum, Germany

H. Kamada

Department of Physics, Faculty of Engineering,

Kyushu Institute of Technology, Kitakyushu 804-8550, Japan

W. N. Polyzou

Department of Physics and Astronomy,

The University of Iowa, Iowa City, IA 52242

(Dated: February 17, 2011)

Abstract

We extend our formulation of relativistic three-nucleon Faddeev equations to include both pairwise interactions and a three-nucleon force. Exact Poincaré invariance is realized by adding interactions to the mass Casimir operator (rest Hamiltonian) of the non-interacting system without changing the spin Casimir operator. This is achieved by using interactions defined by rotationally invariant kernels that are functions of internal momentum variables and single-particle spins that undergo identical Wigner rotations. To solve the resulting equations one needs matrix elements of the three-nucleon force with these properties in a momentum-space partial-wave basis. We present two methods to calculate matrix elements of three-nucleon forces with these properties. For a number of examples we show that at higher energies, where effects of relativity and of three-nucleon forces are non-negligible, a consistent treatment of both is required to properly analyze the data.

PACS numbers: 21.45.-v, 21.45.Ff, 25.10.+s, 24.10.Jv

I. INTRODUCTION

High precision nucleon-nucleon potentials such as AV18 [1], CDBonn [2], Nijm I, II and 93 [3] provide a very good description of the nucleon-nucleon data set up to about 350 MeV. When these forces are used to predict binding energies of three-nucleon systems they underestimate the experimental bindings of ^3H and ^3He by about 0.5-1 MeV [4, 5]. This missing binding energy can be restored by introducing a three-nucleon force into the nuclear Hamiltonian [5].

Also the study of elastic nucleon-deuteron scattering and nucleon induced deuteron breakup revealed a number of cases where the nonrelativistic description using only pairwise forces is insufficient to explain the data. Generally, the studied discrepancies between a theory using only nucleon-nucleon potentials and experiment become larger with increasing energy of the three-nucleon system. Adding a three-nucleon force to the pairwise interactions leads in some cases to a better description of the data. The elastic nucleon-deuteron angular distribution in the region of its minimum and at backward angles is the best studied example [6, 7]. The clear discrepancy in these angular regions at energies up to ≈ 100 MeV nucleon lab energy between a theory using only nucleon-nucleon potentials and the cross section data can be removed by adding a modern three-nucleon force to the nuclear Hamiltonian. Such a three-nucleon force must be adjusted with each nucleon-nucleon potential separately to the experimental binding of ^3H and ^3He [6–8]. At energies higher than ≈ 100 MeV current three-nucleon forces only partially improve the description of cross section data and the remaining discrepancies, which increase with energy, indicate the possibility of relativistic effects. The need for a relativistic description of three-nucleon scattering was also raised when precise measurements of the total cross section for neutron-deuteron scattering [9] were analyzed within the framework of nonrelativistic Faddeev calculations [10]. Nucleon-nucleon forces alone were insufficient to describe the data above ≈ 100 MeV. The effects due to relativistic kinematics considered in [10] were comparable at higher energies to the effects due to three-nucleon forces. These results showed the importance of a study taking relativistic effects in the three nucleon continuum into account.

In [11, 12] the first results on relativistic effects in the three-nucleon continuum have been presented. The dynamics was defined by a three-nucleon center of momentum Hamiltonian or mass operator including only pairwise interactions. The mass operator was used to calculate three-nucleon scattering observables. The input to that approach is a "Lorentz boosted" nucleon-nucleon potential, which generates the nucleon-nucleon t-matrix in a moving frame by solving a standard Lippmann-Schwinger equation. To get the nucleon-nucleon potential in an arbitrary moving frame

one needs the interaction in the two-nucleon center of momentum system, which appears in the relativistic nucleon-nucleon Schrödinger or Lippmann-Schwinger equation. The relativistic Schrödinger equation in the two-nucleon center of momentum system differs from the nonrelativistic Schrödinger equation just by the relativistic form for the kinetic energy. Current realistic nucleon-nucleon potentials are defined and fit by comparing the solution of the nonrelativistic Schrödinger equation to experimental data. Up to now nucleon-nucleon potentials refitted with the same accuracy in the framework of the relativistic nucleon-nucleon Schrödinger equation do not exist. Such refitting can be, however, avoided by solving a quadratic integral equation whose solution is a relativistic potential which is phase-equivalent to a given input high-precision nonrelativistic nucleon-nucleon potential [13]. An alternative equivalent approach towards a relativistic nucleon-nucleon t-matrix in another frame is provided in [14].

In our previous studies with only nucleon-nucleon interactions we found that when the nonrelativistic form of the kinetic energy is replaced by the relativistic one and a proper treatment of the relativistic dynamics is included, the elastic scattering cross section is only slightly influenced by relativity. Only at backward angles and higher energies are the elastic cross sections increased by relativity [11]. It is exactly the region of angles and energies where the effects of three-nucleon forces are also significant [8]. Also, for nucleon-deuteron breakup reactions regions of phase space were found at higher energies of the incoming neutron where relativity significantly changes the breakup cross sections [15, 16]. For some spin observables large effects due to relativity and three-nucleon forces have been reported in nucleon-deuteron breakup for an incoming deuteron energy of 270 MeV, some of which seem to be supported by proton-deuteron data [17]. These observations call for three-nucleon continuum relativistic Faddeev calculations which include three-nucleon forces. Only such consistent calculations should be used to analyze the data in cases when both relativity and three-nucleon force effects are large.

The paper is organized as follows. Sec. II provides the conceptual basis for the choice of the momentum-space representation and the definition of spin in the relativistic context. In Sec. III we summarize the formalism underlying relativistic three-nucleon Faddeev calculations with only nucleon-nucleon interactions, presented in detail in [11, 12]. In Sec. IV we focus on the three-nucleon Faddeev equation with an included three-nucleon force and discuss two methods to compute matrix elements of the three-nucleon force in the partial wave basis used in our relativistic calculations. In Sec. V we apply our formulation to elastic nucleon-deuteron scattering and breakup and show and discuss the results. Sec. VI contains our conclusions and summary. Appendixes A and B formulate three-nucleon forces in the momentum space representation adapted to Poincaré invariance.

II. RELATIVISTIC DYNAMICS

Relativistic invariance of a quantum theory means that the Poincaré group (inhomogeneous Lorentz group) is a symmetry group of the theory. This requires the existence of a unitary representation of the Poincaré group [18]. The Poincaré group has ten generators, six Lorentz generators $J^{\mu\nu}$, and four spacetime translation generators, P^μ. The dynamics of the system is given by the Hamiltonian, $H = P^0$. The Lie algebra has two polynomial invariants,

$$M^2 = -P^\mu P_\mu \qquad W^2 = W^\mu W_\mu \tag{1}$$

where W^μ is the Pauli-Lubanski vector [19]

$$W^\mu := -\frac{1}{2}\epsilon^{\mu\alpha\beta\gamma} P_\alpha J_{\beta\gamma}. \tag{2}$$

It satisfies

$$[P^\mu, W^\nu] = 0, \qquad P^\mu W_\mu = 0, \qquad [W^\mu, W^\nu] = i\epsilon^{\mu\nu\alpha\beta} P_\alpha W_\beta. \tag{3}$$

Equation (1) implies that the Hamiltonian can be expressed in terms of the mass operator, $H = \sqrt{M^2 + P^2}$, where $P^2 := \mathbf{P}^2$. Thus, given a representation for $\mathbf{P}$, the dynamics is defined by the mass operator M, which plays the same role in Poincaré invariant quantum mechanics as the center of mass Hamiltonian $h = H - P^2/2M$ does in Galilean invariant quantum mechanics.

In the absence of interactions the mass operator M becomes the invariant mass operator M_0 of three non-interacting relativistic particles. The full interaction is defined by

$$V := M - M_0. \tag{4}$$

For a system of three particles interacting with short-range interactions, two-body interactions are defined by

$$V_{(ij)(k)} := M_{(ij)(k)} - M_0 \tag{5}$$

where $M_{(ij)(k)}$ is obtained from M by turning off all interactions in M that involve particle k. The difference

$$V_4 := V - V_{(12)(3)} - V_{(23)(1)} - V_{(31)(2)} \tag{6}$$

defines a three-body interaction. With these definitions the mass operator has the form

$$M = M_0 + V_{(12)(3)} + V_{(23)(1)} + V_{(31)(2)} + V_4. \tag{7}$$

This has the same form as the non-relativistic three-body center of mass Hamiltonian with two and three-body forces, except the non-relativistic kinetic energy is replaced by the relativistic invariant mass of the non-interacting system. As in the non-relativistic case, bound and scattering eigenstates of this mass operator can be computed using the Faddeev equations with two and three-body interactions. For identical nucleons the coupled relativistic Faddeev equations can be replaced by a single equation. Details are discussed in the next section.

In addition to the constraints imposed by discrete symmetries, translational invariance, and particle exchange symmetry, there are non-trivial constraints on the interactions due to both the Poincaré symmetry and cluster properties. The constraints on the interaction due to Poincaré invariance come from the commutator

$$[P^j, J^{0k}] = i\delta_{jk}H, \tag{8}$$

which means that interactions appearing in H must be generated by the operators in the commutator. One way to satisfy the constraints due to Poincaré invariance was suggested by Bakamjian and Thomas [20]. Their construction adds interactions to the mass Casimir operator that commute with the spin Casimir operator

$$\mathbf{j}^2 := W^2/M^2. \tag{9}$$

The required interactions commute with and are independent of the total momentum and commute with the non-interacting three-body canonical spin operator.

Spin is associated with rotational degrees of freedom that appear in the rest frame. Because the Lorentz boost generators, J^{0i}, do not form a closed sub-algebra, a sequence of Lorentz boosts that map the rest frame to the rest frame can generate a rotation. Thus in order to obtain a well-defined relativistic spin it is necessary to define a standard procedure for measuring the spin. This normally requires the specification of a special frame where spins can be compared (usually the rest frame) and a standard set of Lorentz transformations $B^{-1}(P)^\mu{}_\nu$, parameterized by momentum, that transform arbitrary frames to the special frame. The three-body canonical spin is defined in terms of the Pauli-Lubanski vector by [21]

$$(0, \mathbf{j}_c)^\mu := \frac{1}{M} B_c^{-1}(P)^\mu{}_\nu W^\nu \tag{10}$$

where $B_c^{-1}(P)^\mu{}_\nu$ is the rotationless Lorentz transformation-valued function of the four momentum P,

$$B_c^{-1}(P)^\mu{}_\nu := \begin{pmatrix} P^0/M & -\mathbf{P}/M \\ -\mathbf{P}/M & I + \frac{\mathbf{P}\otimes\mathbf{P}}{M(P^0+M)} \end{pmatrix}. \tag{11}$$

This Lorentz transformation (11) satisfies

$$B_c^{-1}(P)^\mu{}_\nu P^\nu = (M, \mathbf{0})^\mu. \tag{12}$$

Equations (3) and (12) can be used to show that the components of $\mathbf{j}_c$ satisfy $SU(2)$ commutation relations. The spin $(0, \mathbf{j}_c)^\mu$ is not a four vector because $B_c^{-1}(P)^\mu{}_\nu$ is a matrix of operators, rather than a constant Lorentz transformation. Under Lorentz transformation the canonical spin Wigner rotates

$$(0, \mathbf{j}'_c)^\mu := R_{wc}(\Lambda, P)^\mu{}_\nu (0, \mathbf{j}_c)^\nu \tag{13}$$

where $R_{wc}(\Lambda, P)^\mu{}_\nu := (B_c^{-1}(\Lambda P)\Lambda B_c(P))^\mu{}_\nu$. The spin Casimir operator $\mathbf{j}^2 = \mathbf{j}_c \cdot \mathbf{j}_c$ is independent of the choice of boost (11) used to define the spin. The non-interacting (kinematic) canonical spin, $\mathbf{j}_{c0}$, is obtained from (10) by replacing $M \to M_0$, $W^\mu \to W_0^\mu$ in (10) and $M \to M_0$ in (11). Thus, Poincaré invariance can be satisfied provided the interactions $V_{(ij)(k)}$ and V_4 commute with $\mathbf{j}_{c0}$.

The other non-trivial constraint on the interactions is imposed by cluster properties. The problem arises due to the non-linear relation between the two-body interaction v_{ij} in the two-body problem and the corresponding two-body interaction, $V_{(ij)(k)}$, in the three-body problem. Cluster properties relate $V_{(ij)(k)}$ to the Poincaré generators for the interacting ij pair and spectator k. Unfortunately each $2+1$ mass operator constructed by requiring cluster properties commutes with a different spin Casimir operator, which means that linear combinations of these interactions will break Poincaré invariance. Coester [22] observed that these interactions could be replaced by phase-equivalent interactions that commute with $\mathbf{j}_{c0}$. These interactions are designed to satisfy cluster properties in the three-body rest frame. Using the Bakamjian-Thomas construction linear combinations of the phase equivalent $V_{(ij)(k)}$'s can be added in a manner that preserves the overall Poincaré invariance. While these interactions do not lead to generators that satisfy cluster properties, cluster properties in the three-body rest frame and Poincaré invariance of the S matrix ensures that the three-body S-matrix retains cluster properties in all frames.

To construct two-body interactions, the two-body interactions in the two-body problem that commute with the two-body canonical spin are replaced by phase equivalent two-body interactions in the three-body problem that commute with the three-body canonical spin. The phase equivalent interactions are identified in the rest frame of the three-body system. They are determined in all other frames by the requirement that the three-body spin remains kinematic (in the Bakamjian-Thomas construction this choice fixes the representation of the boost generators).

To construct interactions that commute with the three-body kinematic canonical spin it is useful to introduce momenta and spin variables that have the same Wigner rotation properties

as the three-body kinematic canonical spin. This is because the kinematic canonical spin can be constructed out of these degrees of freedom using conventional methods for adding angular momenta.

The desired momentum operators are the relativistic analog of Jacobi momenta. In the non-relativistic case Jacobi momenta can be defined using Galilean boosts to the two and three-body rest frames. In the relativistic case the Galilean boosts are replaced by the rotationless boost (11) and the relevant Jacobi momenta are [22]

$$q_i^\mu = B_c^{-1}(P)^\mu{}_\nu p_i^\nu \qquad P^\mu = p_1^\mu + p_2^\mu + p_3^\mu \qquad q_i^\mu = (\sqrt{q_i^2 + m^2}, \mathbf{q}_i) \tag{14}$$

$$k_{ij}^\mu = B_c^{-1}(q_{ij})^\mu{}_\nu q_i^\nu \qquad q_{ij}^\mu := q_i^\mu + q_j^\mu. \tag{15}$$

In terms of these variables

$$M_0 = \sum_{i=1}^{3} \sqrt{m^2 + q_i^2} = \sqrt{m_{ij0}^2 + q_k^2} + \sqrt{m^2 + q_k^2} \tag{16}$$

where the two-body invariant mass is

$$m_{ij0} = \sqrt{-(q_i + q_j)^\mu (q_i + q_j)_\mu} = \sqrt{m_i^2 + k_{ij}^2} + \sqrt{m_j^2 + k_{ji}^2}. \tag{17}$$

The vector variables satisfy

$$\sum_{i=1}^{3} \mathbf{q}_i = \mathbf{0} \qquad \mathbf{k}_{ij} + \mathbf{k}_{ji} = \mathbf{0}. \tag{18}$$

The relevant property of these momentum vectors is that they experience the same Wigner rotations as the three-body kinematic canonical spin (13),

$$q_i^\mu \to q_i^{\mu\prime} = (B_c^{-1}(\Lambda P)\Lambda B_c(P) B_c^{-1}(P))^\mu{}_\nu p_i^\nu = R_{wc}(\Lambda, P)^\mu{}_\nu q_i^\nu \ . \tag{19}$$

Similarly,

$$k_{ij}^\mu \to k_{ij}^{\mu\prime} = B_c^{-1}(q'_{ij})^\mu{}_\nu q_i^{\nu\prime} = (B_c^{-1}(R_{wc}(\Lambda, P) q_{ij}) R_{wc}(\Lambda, P))^\mu{}_\nu q_i^\nu =$$

$$(B_c^{-1}(R_{wc}(\Lambda, P) q_{ij}) R_{wc}(\Lambda, P) B_c(q_{ij}))^\mu{}_\nu k_{ij}^\nu = R_{wc}(\Lambda, P)^\mu{}_\nu k_{ij}^\nu \tag{20}$$

where the last line follows from the property of the rotationless boosts (11) that the Wigner rotation of a rotation is the rotation [21]

$$R_{wc}(R, P)^\mu{}_\nu = R^\mu{}_\nu \tag{21}$$

for any $\mathbf{P}$. Thus the $\mathbf{q}_i$ and $\mathbf{k}_{ij}$ all undergo the same Wigner rotations as the three-body kinematic canonical spin.

Next we introduce single-particle spins with the same property. Single-particle canonical spins can be constructed from single-particle Poincaré generators using

$$(0, \mathbf{j}_{ci})^\mu := \frac{1}{m} B_c^{-1}(p_i)^\mu{}_\nu W_i^\nu \tag{22}$$

where the operators on the right side of (22) are constructed by replacing all of the three-body generators in (2), (10) and (11) by the corresponding one-body generators.

Under kinematic Lorentz transformations the single-particle canonical spins experience Wigner rotations, $R_{wc}(\Lambda, p_i)^\mu{}_\nu$, that depend on the single-particle momenta. These rotations differ from the Wigner rotations experienced by $\mathbf{q}_i$, $\mathbf{k}_{ij}$ and $\mathbf{j}_{c0}$. This can be changed by introducing new single-particle spin operators that replace the rotationless boost in (22) by a two step boost,

$$B_c^{-1}(p_i)^\mu{}_\nu \to (B_c^{-1}(q_i) B_c^{-1}(P))^\mu{}_\nu. \tag{23}$$

These two boosts agree when $\mathbf{P} = 0$. Note that both of these boosts transform $p_i^\mu \to (m, 0, 0, 0)^\mu$, so they differ by momentum dependent rotations. We call these spins three-body constituent spins to distinguish them from single-particle canonical spins. The constituent spin operators are defined by [22]

$$(0, \mathbf{j}_{3csi})^\mu := \frac{1}{m} (B_c^{-1}(q_i) B_c^{-1}(P))^\mu{}_\nu W_i^\nu. \tag{24}$$

When $\mathbf{P} = 0$, $B_c^{-1}(p_i) \to B_c^{-1}(q_i)$ which means that single-particle canonical spins and three-body constituent spins agree in the three-body rest frame. For a three-body system the total spin is identified with total angular momentum in the three-body rest frame, which is the sum of the single-particle angular momenta. The angular momentum of a single particle in the three-body rest frame is the sum of the single-particle constituent spin and a contribution from the single particle orbital angular momenta.

A calculation, using the property (21), shows that under Lorentz transformations

$$(0, \mathbf{j}'_{3csi})^\mu := R_{wc}(\Lambda, P)^\mu{}_\nu (0, \mathbf{j}_{3csi})^\nu \ , \tag{25}$$

Wigner rotates with the same rotation as the vectors $\mathbf{q}_i$ and $\mathbf{k}_{ij}$ and the three-body kinematic canonical spin. The three-body kinematic canonical spin is the sum of the orbital angular momenta associated with $\mathbf{q}_k$ and $\mathbf{k}_{ij}$ and the single-particle three-body constituent spins. The requirement that an interaction commutes with the kinematic three-body canonical spin is equivalent to the

requirement that the interaction have a rotationally invariant kernel when expressed in terms of these variables. Thus the required interactions in the Bakamjian-Thomas construction are given by kernels of the form

$$\langle \mathbf{P}, \mathbf{q}_i, \mathbf{k}_{jk}, \mu_1, \mu_2, \mu_3 | V | \mathbf{P}', \mathbf{q}'_i, \mathbf{k}'_{jk}, \mu'_1, \mu'_2, \mu'_3 \rangle = \delta(\mathbf{P} - \mathbf{P}') \langle \mathbf{q}_i, \mathbf{k}_{jk}, \mu_1, \mu_2, \mu_3 \| V \| \mathbf{q}'_i, \mathbf{k}'_{jk}, \mu'_1, \mu'_2, \mu'_3 \rangle \tag{26}$$

where the reduced kernel is a rotationally-invariant function of $\mathbf{q}_i, \mathbf{k}_{jk}$ and the three-body constituent spins.

Two-body interactions in the two-body problem v_{12} have a similar form

$$\langle \mathbf{P}_{12}, \mathbf{k}_{12}, \mu_1, \mu_2 | v_{12} | \mathbf{P}'_{12}, \mathbf{k}'_{12}, \mu'_1, \mu'_2 \rangle = \delta(\mathbf{P}_{12} - \mathbf{P}'_{12}) \langle \mathbf{k}_{12}, \mu_1, \mu_2 \| v_{12} \| \mathbf{k}'_{12}, \mu'_1, \mu'_2 \rangle \tag{27}$$

where

$$k^\mu_{12} = B_c^{-1}(p_1 + p_2)^\mu{}_\nu p_i^\mu \tag{28}$$

is the two-body relative momentum and the magnetic quantum numbers are associated with the two-body constituent spins

$$(0, \mathbf{j}_{2csi})^\mu = \frac{1}{m}(B^{-1}(k_{ij}) B^{-1}(p_i + p_j))^\mu{}_\nu W_i^\nu. \tag{29}$$

When these interactions are embedded in the three-body Hilbert space the kernels (27) are replaced by kernels that are rotationally invariant functions of the three-body Jacobi momenta and the three-body constituent spins. In order to satisfy cluster properties $\mathbf{k}_{ij}$ given by (28) is replaced by the $\mathbf{k}_{ij}$ given by (15), the p_i are replaced by the corresponding q_i, and the two-body constituent spins (29) are replaced by

$$(0, \mathbf{j}_{2(3)csi})^\mu = \frac{1}{m}(B^{-1}(k_{ij}) B^{-1}(q_i + q_j) B^{-1}(P))^\mu{}_\nu W_i^\nu. \tag{30}$$

These operators represent two-body constituent spins in the three-body rest frame. They agree with the two-body constituent spins (29) that they replace in the three-body rest frame, but are defined so they remain unchanged by canonical boosts out of the three-body rest frame. This ensures that they undergo the same Wigner rotations as the kinematic three-body canonical spin under kinematic Lorentz transformations. Thus, the kernels (27) are related by

$$\langle \mathbf{P}, \mathbf{q}_i, \mathbf{k}_{jk}, \mu_1, \mu_2, \mu_3 | v_{jk} | \mathbf{P}', \mathbf{q}'_i, \mathbf{k}'_{jk}, \mu'_1, \mu'_2, \mu'_3 \rangle =$$

$$\delta(\mathbf{P} - \mathbf{P}') \delta(\mathbf{q}_i - \mathbf{q}'_i) \delta_{\mu_i \mu'_i} \sum D^{1/2}_{\mu_j \bar{\mu}_j} [B_c(q_j) B_c(q_j + q_k) B_c(k_{jk})] D^{1/2}_{\mu_k \bar{\mu}_k} [B_c(q_k) B_c(q_j + q_k) B_c(-k_{jk})] \times$$

$$\langle \mathbf{k}_{jk}, \bar{\mu}_j, \bar{\mu}_k \| v_{jk} \| \mathbf{k}'_{jk}, \bar{\mu}'_j, \bar{\mu}'_k \rangle \times$$

$$D^{1/2}_{\bar{\mu}'_j \mu'_j}[B_c^{-1}(k'_{jk}) B_c^{-1}(q'_j + q'_k) B_c^{-1}(q'_j)] D^{1/2}_{\bar{\mu}'_k \mu'_k}[B_c^{-1}(-k'_{jk}) B_c^{-1}(q'_j + q'_k) B_c^{-1}(q'_k)]. \tag{31}$$

Here the unbarred magnetic quantum numbers are three-body constituent spins while the barred magnetic quantum numbers are the two-body constituent spins in the three-body rest frame.

Even though the spins in (30) transform the same way as the three-body constituent spins, they differ from the three-body constituent spins (24) by the Wigner rotation

$$(0, \mathbf{j}_{2(3)ics})^\mu = ((B^{-1}(k_{ij}) B^{-1}(q_i + q_i) B^{-1}(q_i))^\mu{}_\nu (0, \mathbf{j}_{3ics})^\mu. \tag{32}$$

When the two-body interactions are embedded in the three-body system the spins are identified with the two-body constituent spins in the three-body rest frame, as would be expected by cluster properties, but in other frames they are defined to remain unchanged with respect to canonical boosts out of the three-body rest frame. The Wigner rotations (44) and (A2) arise because the two-body subsystem is moving in the three-body rest frame; however because the Wigner rotations in (32) are functions of the q_i rather than the p_i, both spins in (32) undergo the same Wigner rotations under kinematic Lorentz transformation. Because of this it is also possible to construct the three-body canonical spin using partial wave methods directly in a mixed representation involving the barred spins in the interacting pair and the unbarred spin for the spectator. In the mixed representation the two-body interaction in the three-body Hilbert space has the simple form

$$\langle \mathbf{P}, \mathbf{q}_i, \mathbf{k}_{jk}, \bar{\mu}_1, \bar{\mu}_2, \mu_3 | v_{jk} | \mathbf{P}', \mathbf{q}'_i, \mathbf{k}'_{jk}, \bar{\mu}'_1, \bar{\mu}'_2, \mu'_3 \rangle =$$

$$\delta(\mathbf{P} - \mathbf{P}') \delta(\mathbf{q}_i - \mathbf{q}'_i) \delta_{\mu_i \mu'_i} \langle \mathbf{k}_{jk}, \bar{\mu}_j, \bar{\mu}_k \| v_{jk} \| \mathbf{k}'_{jk}, \bar{\mu}'_j, \bar{\mu}'_k \rangle \tag{33}$$

For the two-body problem in the three-body Hilbert space it is advantageous to use (33) because spins (30) do not require Wigner rotations. However, with this choice each interacting pair of particle must be treated using a permuted basis which requires Wigner rotations in the permutation operators. The three-body forces are naturally expressed by a rotationally invariant kernel in the three-body constituent spins. When they are transformed to a mixed basis that involves the spin (30) for one pair, then it is necessary to transform two of the three-body constituent spins with the Winger rotations in (32). The calculations performed in this work use a partial wave projection of the mixed basis (33), although the Wigner rotations in the three body-interaction are not yet included.

III. RELATIVISTIC THREE-NUCLEON FADDEEV EQUATIONS WITH NUCLEON-NUCLEON FORCES

The nucleon-deuteron scattering with neutron and protons interacting through only a nucleon-nucleon interaction v_{NN} is described in terms of a breakup operator T satisfying the Faddeev-type integral equation [23, 24]

$$T|\phi\rangle \;=\; tP|\phi\rangle + tPG_0T|\phi\rangle. \tag{34}$$

The two-nucleon t-matrix t is the solution of the Lippmann-Schwinger equation with the interaction v_{NN}. The permutation operator $P = P_{12}P_{23} + P_{13}P_{23}$ is given in terms of the transposition operators, P_{ij}, which interchanges nucleons i and j. The incoming state $|\phi\rangle = |\mathbf{q}_0\rangle|\phi_d\rangle$ describes the free nucleon-deuteron motion with relative momentum $\mathbf{q}_0$ and the deuteron state vector $|\phi_d\rangle$. Finally G_0 is resolvent of the three-body center of mass kinetic energy. Transition operators for the elastic nd scattering, U, and breakup, U_0, are given in terms of T by [23, 24]

$$\begin{aligned} U &= PG_0^{-1} + PT \;, \\ U_0 &= (1+P)T \;. \end{aligned} \tag{35}$$

This is our standard nonrelativistic formulation, which is equivalent to the nonrelativistic three-nucleon Schrödinger equation plus boundary conditions. The formal structure of these equations in the relativistic case remains the same but the ingredients change. As explained in [25] the relativistic three-nucleon rest Hamiltonian (mass operator) has the same form as the nonrelativistic one, only the momentum dependence of the kinetic energy and the relation of the pair interactions in the three-body problem to the pair interactions in the two-body problem change. Consequently all the formal steps leading to (34) and (35) remain the same.

The free relativistic invariant mass of three identical nucleons of mass m has the form [12] (see Eq.(16))

$$M_0 = \sqrt{m_{230}^2 + q^2} + \sqrt{m^2 + q^2} \tag{36}$$

with spectator momentum $\mathbf{q} := \mathbf{q}_1$ and the free two-body mass operator m_{230} expressed in terms of the relative momentum $\mathbf{k} := \mathbf{k}_{23}$ in the $2-3$ center of momentum frame by (see Eq.(17))

$$m_{230} \equiv 2\sqrt{k^2 + m^2} \equiv 2\omega_m(k) \;. \tag{37}$$

As introduced in [22] and in Eq.(5) the pair forces in the relativistic three-nucleon $2+1$ mass operator are related to the two-body forces in the two-body problem, v_{ij}, by

$$V_{(ij)(k)} = \sqrt{(m_{ij0} + v_{ij})^2 + q^2} - \sqrt{m_{ij0}^2 + q^2} \;, \tag{38}$$

where $V = V(q^2)$ reduces to the interaction v for $\mathbf{q} = 0$, which acts in the two-body center of momentum frame. The momentum dependence ensures that the resulting three-nucleon scattering matrix satisfies space-like cluster properties in all frames [22].

The transition matrix t that appears in the kernel of the Faddeev equation (34) is obtained by solving the relativistic Lippmann-Schwinger equation as a function of q^2

$$t(\mathbf{k},\mathbf{k}';q^2) \;=\; V(\mathbf{k},\mathbf{k}';q^2) + \int d^3k'' \frac{V(\mathbf{k},\mathbf{k}'';q^2)t(\mathbf{k}'',\mathbf{k}';q^2)}{\sqrt{(2\omega_m(k'))^2+q^2} - \sqrt{(2\omega_m(k''))^2+q^2}+i\epsilon}. \tag{39}$$

The input two-body interaction V is computed by solving the nonlinear equation [13]

$$\{\sqrt{m_{ij0}^2+q^2}, V_{(ij)(k)}\} + V_{(ij)(k)}^2 = 4mv_{NN}\ , \tag{40}$$

where v_{NN} is a nonrelativistic nucleon-nucleon potential fitted to the nucleon-nucleon data basis and where anticommutator $\{A,B\} \equiv AB + BA$. In case of $\mathbf{q} = \mathbf{0}$ that equation reduces to a nonlinear equation for the relativistic two-body interaction v. Therefore the problem of refitting all two-nucleon data when changing from a nonrelativistic to a relativistic Lippmann-Schwinger equation is avoided. The nonlinear equation (40) can be solved by iteration [13]. An alternative approach to determine $t(\mathbf{k},\mathbf{k}';q^2)$ is described in [14].

The new relativistic ingredients in (34) and (35) will therefore be the t-operator (39) (expressed in partial waves) and the resolvent of the three-nucleon invariant mass

$$G_0 \;=\; \frac{1}{E+i\epsilon-M_0}, \tag{41}$$

with M_0 given by (36). E is the total three-nucleon invariant mass expressed in terms of the initial neutron momentum $\mathbf{q}_0$ relative to the deuteron by

$$E \;=\; \sqrt{M_d^2+{q_0}^2} + \sqrt{m^2+{q_0}^2}, \tag{42}$$

with M_d the deuteron rest mass. Related to the choice of the permutation operator P the pair $i-j$ is chosen as $2-3$.

Currently the Faddeev equation (34) in its nonrelativistic form is numerically solved for any nucleon-nucleon interaction using a momentum space partial-wave decomposition. Details are presented in [23]. Projecting (34) on such a basis turns it into a coupled set of two-dimensional integral equations. As shown in [11, 12], in the relativistic case we can keep the same formal structure, though the permutation operators are replaced by the corresponding Racah coefficients for the Poincaré group which include both Jacobians and Wigner rotations that do not appear in the nonrelativistic permutation operators [24, 26].

In the nonrelativistic case the partial-wave projected momentum-space basis is

$$|pq(ls)j(\lambda\frac{1}{2})IJ(t\frac{1}{2})T\rangle, \tag{43}$$

where p and q are the magnitudes of standard Jacobi momenta (see [24, 26]), obtained by transforming single particle momenta to the rest frame of a two- or three-body system using a Galilean boost, and $(ls)j$ are two-body quantum numbers with obvious meaning, $(\lambda 1/2)I$ refer to the third, spectator nucleon, taken as the nucleon 1 and described by the momentum q, J is the total three-nucleon angular momentum and the rest are isospin quantum numbers. In the relativistic case this basis is replaced by the Poincaré irreducible states defined as [12]

$$\begin{aligned}
&\langle \mathbf{p}_1,\mu_1',\mathbf{p}_2,\mu_2',\mathbf{p}_3,\mu_3'|(J,q)\mathbf{P}=\mathbf{0},\mu;\lambda,I,j_{23},k_{23},l_{23},s_{23}\rangle \;= \\
&\delta(\mathbf{0}-\mathbf{q}_1-\mathbf{q}_2-\mathbf{q}_3)\frac{1}{N(q_2,q_3)}\frac{\delta(q_1-q)}{q^2}\frac{\delta(k(\;\mathbf{q}_2,\mathbf{q}_3\;)-k)}{k^2} \\
&\sum_{\mu_2\mu_3\mu_s}\sum_{\mu_l\mu_\lambda\mu_I}(\frac{1}{2},\mu_2,\frac{1}{2},\mu_3|s,\mu_s)(l,\mu_l,s,\mu_s,|j,\mu_j)(\lambda,\mu_\lambda,\frac{1}{2},\mu_1'|I,\mu_I)(j,\mu_j,I,\mu_I|J,\mu) \\
&Y_{\lambda\mu_\lambda}(\hat{\mathbf{q}}_1)Y_{l\mu_l}(\hat{\mathbf{k}}(\mathbf{q}_2,\mathbf{q}_3))D^{\frac{1}{2}}_{\mu_2'\mu_2}[R_{wc}(B_c(-q_1),k_2(\mathbf{q}_2,\mathbf{q}_3))]D^{\frac{1}{2}}_{\mu_3'\mu_3}[R_{wc}(B_c(-q_1),k_3(\mathbf{q}_2,\mathbf{q}_3))]\;,
\end{aligned} \tag{44}$$

where $N(q_2,q_3)$ is given by (A3) in Appendix A and $\vec{k}(\vec{q}_2,\vec{q}_3)$ by (B1) in Appendix B. These states are labeled by the same quantum numbers as the corresponding non-relativistic basis states.

The basis states (44) are used for the evaluation of the partial wave representation of the permutation operator P with Wigner rotations of spin states for nucleons 2 and 3 included. In the relativistic case we adopt the following short-hand notation for the Poincaré irreducible three-body states, which also includes isospin quantum numbers coupled in the same order:

$$|k,q,\alpha\rangle := |kq(ls)j(\lambda,\frac{1}{2})IJ(t\frac{1}{2})T\rangle = |(J,q)\mathbf{P}=\mathbf{0},\mu;\lambda,I,j_{23},k_{23},l_{23},s_{23}\rangle|(t\frac{1}{2})T\rangle\;. \tag{45}$$

Equipped with that, projecting (34) onto the basis states $|k,q,\alpha\rangle$ one encounters, using the non-relativistic notation of Ref. [26]

$${}_1\langle kq\alpha|P|k'q'\alpha'\rangle_1 \;=\; {}_1\langle kq\alpha|k'q'\alpha'\rangle_2 + {}_1\langle kq\alpha|k'q'\alpha'\rangle_3 = 2\;{}_1\langle kq\alpha|k'q'\alpha'\rangle_2. \tag{46}$$

This is evaluated by inserting the complete basis of single-particle states $|\mathbf{p}_1,\mu_1,\mathbf{p}_2,\mu_2,\mathbf{p}_3,\mu_3\rangle$ and using (44). It can be expressed in a form which resembles closely the corresponding non-relativistic expression [24, 26]

$$\begin{aligned}
{}_1\langle k\;q\;\alpha|\;P\;|k'\;q'\;\alpha'\rangle_1 \;=\; &\int_{-1}^{1}dx\frac{\delta(k-\pi_1)}{k^2}\;\frac{\delta(k'-\pi_2)}{k'^2} \\
&\frac{1}{N_1(q,q',x)}\;\frac{1}{N_2(q,q',x)}\;G^{BB}_{\alpha\alpha'}(q,q',x),
\end{aligned} \tag{47}$$

where all ingredients are defined in Appendix A2 of Ref. [12]. The rotational invariance of the nucleon-nucleon interaction in this basis ensures that all three nucleon-nucleon interactions commute with the spin Casimir operator of the non-interacting three-nucleon system. This allows the interactions to be added in a manner that preserves the underlying Poincaré symmetry.

Due to the short-range nature of the nucleon-nucleon interaction it can be considered negligible beyond a certain value j_{max} of the total angular momentum in the two-nucleon subsystem. Generally with increasing energy j_{max} will also increase. For $j > j_{max}$ we set the t-matrix to zero, which yields a finite number of coupled channels for each total angular momentum J and total parity $\pi = (-)^{l+\lambda}$ of the three-nucleon system. To achieve converged results at incoming nucleon laboratory energies below ≈ 250 MeV all partial wave states with total angular momenta of the two-nucleon subsystem up to $j_{max} = 5$ and all total angular momenta of the three-nucleon system up to $J = 25/2$ must be taken into account. This leads to a system of up to 143 coupled integral equations in two continuous variables for a given J and parity. For the details of the numerical performance we refer to [11, 24, 26]. The solution of these equations can be used to construct an exactly Poincaré invariant scattering operator.

IV. RELATIVISTIC THREE NUCLEON FADDEEV EQUATIONS WITH A THREE-NUCLEON FORCE INCLUDED

In the standard nonrelativistic formulation when in addition to pairwise interactions v_{NN} between three nucleons also a three-nucleon force is included, a new term V_4 appears in a potential energy of the three-nucleon system

$$V_4 = V_4^{(1)} + V_4^{(2)} + V_4^{(3)} \ . \tag{48}$$

Each $V_4^{(i)}$ is symmetric under exchange of the nucleons j and k ($i, j, k = 1, 2, 3$ and $j \neq i \neq k$). In the 2π-exchange three-nucleon force $V_4^{(1)}$ is a contribution to the three-nucleon potential from (off-shell) rescattering of a pion on nucleon 1.

When a three-nucleon force is acting then on top of rescatterings among three nucleons induced by pairwise forces only, which are summed up in integral equation (34), additional rescatterings induced by three-nucleon force and nucleon-nucleon force appear.

Therefore Faddeev equation (34) changes to

$$T|\phi\rangle = \ t\,P\,|\phi\rangle \ + \ (1+tG_0)\,V_4^{(1)}\,(1+P)\,|\phi\rangle \ + \ t\,P\,G_0\,T|\phi\rangle \ + \ (1+tG_0)\,V_4^{(1)}\,(1+P)\,G_0\,T|\phi\rangle \ , \tag{49}$$

with one new contribution in the leading term and in the kernel [24, 27]. While the breakup transition operator U_0 preserves its form (35), in the elastic scattering operator U two new contributions appear [24, 27]

$$U = PG_0^{-1} \; + \; V_4^{(1)}\,(1+P) \; + \quad PT \; + \; V_4^{(1)}\,(1+P)\,G_0\,T \; . \tag{50}$$

The second term is due to a single interaction of three-nucleons via a three-nucleon force and the fourth results from rescattering among three nucleons induced by two- and three-nucleon forces with a three-nucleon force as the final interaction.

After projecting on a partial-wave momentum-space basis equation (49) becomes a system of 2-dimensional coupled integral equations which can be solved numerically exactly for any nuclear force. Since the three-nucleon force is short-ranged its inclusion needs to be carried through only for all total angular momenta of the three nucleon system up to $J = 13/2$. As mentioned in section III, the longer ranged two-nucleon interactions require states up to $J = 25/2$. For details of the formalism and numerical performance in case of the nonrelativistic formulation when three-nucleon force is included we refer to Refs. [23, 24, 28].

For relativistic calculations without a three-nucleon force, briefly described in previous section, the details of the numerical treatment are given in [11, 12]. When a three-nucleon force is added two new terms in (49) contain the free three-nucleon propagator G_0. Since in the basis $|\mathbf{k}, \mathbf{q}>$ (see Appendix B) the three-nucleon invariant mass M_0 is diagonal, G_0 is given by

$$\langle \mathbf{k}, \mathbf{q}|G_0|\mathbf{k}', \mathbf{q}'\rangle = \delta(\mathbf{k}-\mathbf{k}')\delta(\mathbf{q}-\mathbf{q}')\frac{1}{E - \sqrt{m^2+q^2} - \sqrt{4(k^2+m^2)+q^2} + i\epsilon} \; . \tag{51}$$

That means that performing integrations over momenta k' and q' in the intermediate states $|k', q', \alpha'\rangle$ during the calculation of matrix elements for these new terms, the simple pole singularity occurs for momenta $q' < q_{max}$ at $k' = k_0$, where q_{max} is given by the total three-nucleon center of momentum energy E through $E = \sqrt{4m^2 + q_{max}^2} + \sqrt{m^2 + q_{max}^2}$.

For a given q'-value the momentum k_0 is the solution of $E = \sqrt{4(m^2 + k_0^2) + q'^2} + \sqrt{m^2 + q'^2}$. The treatment of that pole, as well as of the deuteron bound state pole in T, which occurs at $q' = q_0$ for channels α' containing the deuteron quantum numbers, was done using subtraction method [23, 24].

The nonrelativistic treatment of (49) requires matrix elements of $V_4^{(1)}(1+P)$ calculated in a partial-wave basis with standard Jacobi momenta: $\langle p, q, \alpha|V_4^{(1)}(1+P)|p', q', \alpha'\rangle$. In the relativistic calculations, however, one needs them in the new, relativistic basis $|k, q, \alpha\rangle$. The generation of three-nucleon force partial-wave matrix elements is the most time consuming part of three-nucleon

continuum Faddeev calculations. One way to reduce the computer time is to perform a transformation of the existing, standard Jacobi momenta matrix elements to the relativistic basis. In Appendix A we give the expression (A17) for such transformation which is valid in the general case, when in addition to boost also Wigner spin rotations are taken into account. The complex structure of that transformation, where in addition to the summation over numerous intermediate states with geometrical coefficients, also involved are two integrations and two interpolations over the momenta p and p', prevents, due to the large amount of computing time and computer resources required, the application of that transformation in fully converged calculations.

It seems thus unavoidable that in order to get matrix elements $\langle k, q, \alpha | V_4^{(1)} | k', q', \alpha' \rangle$ one must start from a commonly given expression for a three-nucleon force in terms of individual nucleons momenta and their spin and isospin operators and to apply to that expression the recently proposed automatized partial wave decomposition [29, 30]. To that aim we derived in Appendix B relation (B4) which allows to express matrix element of a three-nucleon force in a 3-dimensional relativistic basis $\langle \mathbf{k}, \mathbf{q} | V_4^{(1)} | \mathbf{k}', \mathbf{q}' \rangle$ by its matrix element in the individual nucleons momenta basis. In this basis $\mathbf{q}$ and $\mathbf{k}$ undergo identical Wigner rotations under kinematic boost of the three-nucleon system. The nucleon spins are defined to be the three-body constituent spins (canonical spins measured by using a rotationless boost to the three-body center of momentum frame). To use them in the $|k, q, \alpha\rangle$ basis the spins for the α pair must be Wigner rotated before they are coupled. The alternative is to use the representation where three spins are three-body constituent spins; in this case all three of the two-body interactions will have Wigner rotations that convert the two-body constituent spins in the three body rest frame to three-body constituent spins. The three-nucleon force will have no Wigner rotations. In this representation all of the spins can be coupled using standard partial wave methods. For our calculations we work in the $|k, q, \alpha\rangle$ basis, but do not account for the Wigner rotations in the three-nucleon interaction for the reasons discussed in the previous paragraph. This allows us to treat the spins in the three-nucleon force using conventional methods. This assumes the Wigner rotations in the three-nucleon force can be neglected. Neglecting these Wigner rotations has no effect on the relativistic invariance or S-matrix cluster properties.

V. RESULTS

To study the importance of a consistent treatment of both relativity and a three-nucleon force we numerically solved the three-nucleon Faddeev equations for neutron-deuteron scattering at the neutron laboratory energies $E_n^{lab} = 70$, 135, 200 and 250 MeV. As dynamical input we took the

nonrelativistic nucleon-nucleon potential CD Bonn [2] and TM99 three-nucleon force [31–33]. The cut-off parameter Λ of that three-nucleon force was adjusted to $\Lambda = 4.469$ in units of the pion mass, m_π, to give, together with the CD Bonn potential, the experimental binding energy of ^{3}H. At each energy we generated solutions of nonrelativistic and relativistic three-nucleon Faddeev equation, without and with TM99 three-nucleon force included. For relativistic case we produced, starting from the CD Bonn potential and solving nonlinear equation (40) at the required spectator nucleon momenta q, the relativistic, on-shell equivalent interaction with boost effects incorporated exactly. That interaction served as dynamical input to calculate, using the relativistic Lippmann-Schwinger equation (39) the relativistic off-shell t-matrix t that appears in Faddeev equations.

Since in [12] it was found that effects of Wigner spin rotations are practically negligible in the studied energy range, we neglected them in the present study. When performing relativistic calculations with three-nucleon force included one requires matrix elements of the TM99 three-nucleon force in a relativistic momentum space basis, where the relative momentum of two nucleons in their c.m. system, $\mathbf{k}$, replaces standard Jacobi momentum $\mathbf{p}$. That momentum $\mathbf{k}$ together with spectator nucleon momentum $\mathbf{q}$, equal in magnitude and opposite to the total momentum of the free pair in three-nucleon center of momentum system, unambiguously define the configuration of three nucleons. Since it is the region of small and not large momenta which is most important when solving Faddeev equations it seems reasonable to assume that the momenta $\mathbf{k}$ and $\mathbf{p}$ do not differ substantially. Therefore, in order to avoid calculations of the TM99 three-nucleon force matrix elements in a relativistic basis $|k, q, \alpha\rangle$ we assumed, that the matrix elements in a relativistic and nonrelativistic bases are equal:

$$\langle k, q, \alpha | V_4^{(1)} | k', q', \alpha' \rangle \;=\; \langle p = k, q, \alpha | V_4^{(1)} | p' = k', q', \alpha' \rangle \; . \tag{52}$$

That assumption allowed us to use the existing matrix elements of the TM99 three-nucleon force.

To check quality of the approximation (52) we compared the matrix element of the TM99 3NF in the relativistic basis, $\langle k, q, \alpha | V_4^{(1)} | k', q', \alpha' \rangle$, calculated according to (B4) and using automatized partial wave expansion of Ref. [30] (what corresponds to neglection of Wigner spin rotations in (B5)), with the corresponding matrix element in the standard, nonrelativistic basis, $\langle p, q, \alpha | V_4^{(1)} | p', q', \alpha' \rangle$, at a number of the spectator momentum values. In Figs. 1 and 2 we exemplify the typical behavior showing at a number of q' values and at a fixed $p = k$, taking two different values of q, the $k' (= p')$ dependence of these matrix elements for a particular channel $\alpha = \alpha' = |(00)0(0\frac{1}{2})\frac{1}{2}(1\frac{1}{2})\frac{1}{2} >$. As expected, clear differences between these matrix elements occur only at very large values of the spectator momentum q, where magnitudes of these matrix elements

are small. This justifies application of the approximation (52) in the present study.

The approximation (52) can be investigated also directly for the three-dimensional matrix elements, comparing $\langle \mathbf{k}, \mathbf{q} \mid V_4^{(1)} \mid \mathbf{k}', \mathbf{q}' \rangle$ and $\langle \mathbf{p}, \mathbf{q} \mid V_4^{(1)} \mid \mathbf{p}', \mathbf{q}' \rangle$. The connection between these matrix elements is given by (B4) in Appendix B. They depend on momentum vectors and spin-isospin quantum numbers in the initial and final state. In Fig. 3 we show a particularly simple case, where $t = t' = 0$, all four momenta are parallel to the unit vector $\left(\frac{1}{\sqrt{3}}, \frac{1}{\sqrt{3}}, \frac{1}{\sqrt{3}}\right)$ and all spin magnetic quantum numbers are equal $\frac{1}{2}$. We display $\langle \mathbf{k}, \mathbf{q} \mid V_4^{(1)} \mid \mathbf{k}, \mathbf{q} \rangle$ and $\langle \mathbf{p}, \mathbf{q} \mid V_4^{(1)} \mid \mathbf{p}, \mathbf{q} \rangle$ for several q values as a function of k. We see how the difference develops gradually with increasing q, resembling the picture seen for partial wave decomposed matrix elements.

Transition amplitudes for elastic neutron-deuteron scattering and breakup based on that set of four solutions of three-nucleon Faddeev equations, are used to predict numerous observables for both reactions. By comparing these observables conclusions on how strongly three-nucleon force effects depend on relativity were drawn. In the following subsections we show and discuss results for the cross section and numerous spin observables, separately for elastic scattering and breakup reactions.

A. Elastic scattering

At higher energies of the incoming nucleon three-nucleon forces play significant role in determining the angular distribution of the elastic neutron deuteron scattering. The clear evidence of three-body force effects start to develop at $E_n^{lab} \approx 65$ MeV for scattering angles close to a minimum of the cross section, which at 65 MeV occurs at $\theta_{c.m.} \approx 105^o$ [6, 8]. With increasing energy of the three-nucleon system not only the magnitude of predicted three-nucleon force effect increases but it also influences the cross section in a wider range of angles, which at 250 MeV covers $90^o \leq \theta_{c.m.} \leq 180^o$ [6, 8]. The standard 2π-exchange three-nucleon forces, such as TM99 [33] or Urbana IX [34], are able to account for existing discrepancies between theoretical cross sections obtained with realistic nucleon-nucleon potentials and data only up to $E_n^{lab} \approx 135$ MeV. Data at larger energies in a region of angles ranging from the cross section minimum up to 180^o are drastically underestimated even when 2π-exchange three-nucleon forces are included in the calculations. This is exemplified on Fig. 4, where solid (red) lines are nonrelativistic predictions based on the CD Bonn potential alone and dotted (blue) lines are results obtained when the CD Bonn potential was combined with the TM99 three-nucleon force.

Since effects of relativity for predictions based on two-nucleon forces only are restricted to very

backward angles $\theta_{c.m.} \geq 160^o$ [11] (see also Fig. 4 where dashed (blue) lines are relativistic predictions based on the CD Bonn potential), the drastic discrepancy between data and theory seen at 250 MeV would indicate that at such large energies shorter-ranged three-nucleon force components, not taken into account in these calculations, start to play significant role. The possibility, that including such three-nucleon force contributions would indeed help to improve description of the cross section data is further supported by an interesting pattern revealed when the TM99 three-nucleon force is included into relativistic calculations. Namely, when a consistent treatment of relativity and a three-nucleon force as described in the present study is made, then the resulting changes of the cross section are not a simple incoherent sum of effects due to relativity, seen when two-nucleon forces alone are acting, and three-nucleon force effects found in nonrelativistic calculations. The relativity modulates effects exerted by the TM99 three-nucleon force on the cross section found in nonrelativistic calculations and the magnitude of this modulation depends from the scattering angle. While at backward angles the nonrelativistic cross section with a three-nucleon force included is further enhanced by relativity, in a region of center of momentum angles near the cross section minimum the magnitude of three-nucleon force effects seen in nonrelativistic calculations is strongly reduced by relativity (dashed-dotted (brown) lines in Fig. 4).

Also elastic scattering polarization observables reveal such incoherent and angle-dependent modulation of three-nucleon force effects by relativity. The details, however, depend on the particular spin observable under study and every conceivable scenario can be found.

For elastic scattering spin observables effects of relativity, when only two nucleon forces are acting, were found to be small [11]. It is exemplified by nearly overlapping solid (red) and dashed (blue) lines in Figs. 5-15. Adding three-nucleon force in nonrelativistic calculations leads to substantial effects for some polarization observables, especially at higher energies [7, 8]. The resulting picture, however, is quite complex. Some of those three-nucleon force effects are supported by the data. For some observables they deteriorate the data description.

For tensor analyzing powers A_{xx}, A_{yy} and A_{xz} relativistic effects are non-negligible even at 70 MeV (see Fig. 5) and clearly increase with increasing energy as seen in Figs. 6, 7 and 9. When three-nucleon force is added in the relativistic calculations the resulting effect depends on the observable and the energy.

For A_{xz} large three-nucleon force effects remain. At 70 MeV and 135 MeV they are practically identical in magnitude to three-nucleon force effects found in nonrelativistic calculations and nonrelativistic and relativistic predictions for A_{xz} at these energies are practically overlapping (see dotted (blue) and dashed-dotted (brown) lines in Figs. 5, 6 and 9). At 200 MeV, however,

adding three-nucleon force in relativistic calculations leads to angle dependent modulations of the magnitude of three-nucleon force effects, similar to that found for the cross section (see Fig. 9).

For A_{xx} a drastically different scenario occurs. Large effects of the TM99 three-nucleon force are seen for that observable in nonrelativistic calculations at 70 MeV and 135 MeV in wide range of angles and they practically vanish when relativity is included. As a result the dashed-dotted (brown) line practically overlaps with pure two-nucleon relativistic and nonrelativistic predictions (see Fig. 5 and 6).

For A_{yy} (Fig. 5 and 6) the large effects of the three-nucleon force seen in nonrelativistic calculations are simply reduced by relativity. For the tensor analyzing power A_{zz}, for which data exist only at 135 and 200 MeV, the influence of relativity induces both modulation and reduction of nonrelativistic three-nucleon force effects (Fig. 7).

The TM99 three-nucleon force acts differently on the nucleon, $A_y(N)$, and deuteron, $A_y(d)$, vector analyzing powers. While three-nucleon force effects for $A_y(N)$ are rather small even at 250 MeV (Fig. 8 and 15), for $A_y(d)$ they are significant (Fig. 5, 6 and 8). For $A_y(N)$ and $A_y(d)$, but more clearly displayed due to larger effects for the deuteron vector analyzing power, both reduction and modulation of nonrelativistic three-nucleon force effects by relativity was found. That reduction and modulation depend on angle and energy.

A similar picture was found for numerous spin correlation coefficients, as exemplified by different theoretical predictions shown in Figs. 9-13. Again all scenarios are available: total reduction by relativity of large three-nucleon force effects seen in nonrelativistic calculations (e.g. $C_{x,x}$ at 135 and 200 MeV for $120^o \leq \theta_{c.m.} \leq 150^o$ in Fig. 10, $C_{y,y}$ at 135 and 200 MeV at $120^o \leq \theta_{c.m.} \leq 150^o$ in Fig. 11), practically the same three-nucleon force effects in nonrelativistic and relativistic calculations ($C_{z,z}$ at 135 MeV in Fig. 9, $C_{xz,y}$ at 135 and 200 MeV in Fig. 12), angle dependent modulation of nonrelativistic three-nucleon force effects by relativity ($C_{x,z}$ at 135 MeV in Fig. 9, $C_{z,x}$ at 135 and 200 MeV in Fig. 10, $C_{xy,x}$ and $C_{yz,x}$ at 135 and 200 MeV in Fig. 13).

The polarization transfer coefficients are not exceptions; also for them a similar complex influence of relativity on nonrelativistic three-nucleon force effects have been found as shown in Figs. 14 and 15.

The comparison of nonrelativistic predictions based on 2π-exchange three-nucleon force's revealed for spin observables a complex, angle and energy dependent pattern of discrepancies between data and theory [7, 8, 35–37]. The nontrivial interplay between the 2π-exchange three-nucleon forces and relativity suggests that the inclusion of further three-nucleon force mechanisms, like forces of shorter range, is needed to improve the description of elastic scattering polarisation data.

B. Breakup

Theoretical study of exclusive breakup reaction performed at different incoming nucleon energies revealed regions of breakup phase-space where large three-nucleon force effects have been found [38]. The effects, similarly to elastic scattering, generally increase with energy. With increasing energy also the effects of relativity increase [15, 16], revealing for exclusive breakup cross section a characteristic pattern when viewed as a function of the angles of detected nucleons. Largest effects where found when two of three outgoing nucleons are detected coplanarly on both sides of the beam. Keeping one of the detectors at a constant position and changing the polar angle of the second, regions of phase space were found in which nonrelativistic breakup cross section was increased or decreased by relativity [16]. In these specific configurations effects of three-nucleon force's on breakup cross section, both in norelativistic as well as in relativistic calculations, are practically negligible (see Fig. 16).

Due to richness of the breakup phase-space also geometrical configurations can be found where both, three-nucleon force and relativistic effects are significant. Exclusive cross sections in some of these configurations are shown as a function of the laboratory energy of one of the outgoing and detected nucleons in Fig. 17 for neutron-deuteron breakup at 200 MeV. It is seen that including relativity reduces slightly the magnitude of three-nucleon force effects observed in nonrelativistic calculations.

Relativity changes also the magnitude of three-nucleon force effects seen in nonrelativistic calculations for breakup polarization observables. We exemplify that in Fig. 18 at three configurations of exclusive dp breakup at $E_d^{lab} = 270$ MeV, for which data have been taken [17]. Again, influence of relativity on magnitude of three-nucleon force effects change with configuration as shown in Fig. 18 along the S-curve arc length. Especially interesting is the case of polarization-transfer coefficient from the deuteron to the nucleon, $K_{yy}^{y'}$, for which inclusion of TM99 three-nucleon force changes completely the S-dependence found in case when only two nucleon-forces were acting. The effect of three-nucleon force is further modified slightly by relativity resulting in a better reproduction of data.

VI. SUMMARY AND OUTLOOK

We extended our relativistic formulation of three-nucleon Faddeev equations to include also three-nucleon force. The relativistic features are the relativistic form of the free propagator, the

change of the nucleon-nucleon potential caused by the boost of the two nucleon subsystem, and the modification of the permutation operators. In present study we neglected Wigner spin rotations induced by these boosts since investigations based on two-nucleon forces only have shown that their effects are negligible. For the momentum-space basis we used the relative momentum of two free nucleons in their c.m. system together with their total momentum in the three nucleon c.m. system, which in this frame is the negative momentum of the spectator nucleon. Such a choice of momenta is adequate for relativistic kinematics and allows to generalize the nonrelativistic approach used to solve the nonrelativistic three nucleon Faddeev equation to the relativistic case in a more or less straightforward manner. That relative momentum in the two-nucleon subsystem is a generalization of the standard nonrelativistic Jacobi momentum $\mathbf{p}$. We numerically solved these equations for neutron-deuteron scattering including relativistic features and/or three-nucleon force at the neutron lab energies $E_n^{lab} = 70$, 135, 200 and 250 MeV. As dynamical input we took the nonrelativistic nucleon-nucleon potential CD Bonn and generated in the two nucleon center of momentum system an exactly on-shell equivalent relativistic interaction. As a three-nucleon force we took the 2π-exchange TM99 force.

By comparing our relativistic calculations without and with the three-nucleon force included we studied influence of relativity on three-nucleon force effects. In studies with two-nucleon forces only it was found that significant relativistic effects for the elastic scattering cross section appear at higher energies and they are restricted only to the very backward angles where relativity increases the nonrelativistic cross section. At other angles the effects are small. Also for spin observables, analyzing powers, spin correlation coefficients and spin transfer coefficients, no significant changes due to relativity have been found when only two-nucleon forces were acting. The similar picture was found for breakup, however, in that case significantly larger effects for the cross section in specific regions of the breakup phase-space have been found.

The results obtained in the present study document that this picture changes dramatically when in addition to the two-nucleon force in a relativistic treatment also a three-nucleon force is acting. For the elastic scattering large changes of the cross section at higher energies, caused by three-nucleon force in large region of angles ranging from around minimum of the cross section up to very backward angles, are further significantly modulated by relativity. Also such modulation in a large, similar to that for the cross section, range of angles have been found for numerous polarization observables. In that case every conceivable scenario of modulations was observed: from wiping out large three-nucleon force effects found in nonrelativistic calculations to their modulations with energy and angle, with strong amplification or reduction of their magnitude. Also for exclusive

breakup cross section and polarisation breakup observables in some geometries the relativity influences effects induced by three-nucleon forces. Thus also for that reaction the relativistic treatment when three-nucleon forces are acting is required for proper interpretation of data.

The comparison of our nonrelativistic theory with existing elastic scattering cross section and polarisation data exhibits at the higher energies clear discrepancies. The discrepancies between the theory based on pairwise forces only and data are largest in the region starting from the cross section minimum around $\theta_{c.m.} \approx 130^\circ$ up to $\theta_{c.m.} \approx 180^\circ$. At energies up to about ≈ 135 MeV these discrepancies can be removed when current three-nucleon forces, mostly of 2π-exchange character [31, 34], are included in the nuclear Hamiltonian. At the higher energies, however, a significant part of the discrepancy remains and increases further with increasing energy. Especially complex picture exists for spin observables. Here adding 2π-exchange three-nucleon force into nonrelativistic calculations leads to effects which depend on observable. They can be large or negligible, change their magnitude with energy and angle. Similarly to the elastic scattering cross section even after inclusion of three-nucleon force some of the discrepancies remain and increase with increasing energy. This indicates that additional three nucleon forces should be added to the 2π-exchange type forces. Natural candidates in the traditional meson-exchange picture are exchanges like $\pi - \rho$ and $\rho - \rho$. This has to be expected since in χPT [39] in the order in which nonvanishing three-nucleon force's appear the first time there are three topologies of forces, the 2π-exchange, a one-pion exchange between one nucleon and a two-nucleon contact interaction and a pure three nucleon contact interaction. They are of the same order and have to be kept together. Therefore it appears very worthwhile to pursue a strategy adding in the traditional meson exchange picture further three nucleon forces. Results presented here show that relativistic effects based on relativistic kinematics and boost effects of the nucleon-nucleon force play an important role in building up the magnitude of three-nucleon force effects. That gives hope, that taking the proper three-nucleon force into relativistic Faddeev calculations one will be able to improve the description of higher energy data for cross section and polarization observables.

Acknowledgments

This work has been supported by the Polish 2008-2011 science funds as the research project No. N N202 077435, by the Helmholtz Association through funds provided to the virtual institute "Spin and strong QCD"(VH-VI-231), and by the European Community-Research Infrastructure Integrating Activity "Study of Strongly Interacting Matter" (acronym HadronPhysics2, Grant

Agreement n. 227431) under the Seventh Framework Programme of EU. W. P. is supported by the U.S. Department of Energy, contract DE-FG02-86ER40286. H. W. would like to thank the Kyushu University for hospitality and support during his stay in this institution. The numerical calculations were performed on the supercomputer cluster of the JSC, Jülich, Germany.

Appendix A: Direct recalculation of the partial-wave projected three-nucleon force matrix elements from (p,q)- to (k,q)- based basis

We start from the matrix element of a three-nucleon force $\left\langle p,q,\alpha|V_4^{(1)}(1+P)|p',q',\alpha'\right\rangle$ in a partial wave basis used in norelativistic calculations with standard Jacobi momenta (p,q) [26] and would like to get the matrix element $\left\langle k,q,\alpha|V_4^{(1)}(1+P)|k',q',\alpha'\right\rangle$ with p and p' replaced by the relative momenta of nucleons 2 and 3, k and k', in their two-nucleon center of momentum system [11, 12].

Using completeness of partial wave states one has

$$\begin{aligned}\left\langle k,q,\alpha|V_4^{(1)}(1+P)|k',q',\alpha'\right\rangle \;=\; \sum_{\tilde\alpha}\int d\tilde p\tilde p^2\int d\tilde q\tilde q^2\sum_{\tilde\alpha'}\int d\tilde p'\tilde p'^2\int d\tilde q'\tilde q'^2\,\langle k,q,\alpha|\tilde p,\tilde q,\tilde\alpha\rangle \\ \left\langle \tilde p,\tilde q,\tilde\alpha|V_4^{(1)}(1+P)|\tilde p',\tilde q',\tilde\alpha'\right\rangle\langle\tilde p',\tilde q',\tilde\alpha'|k',q',\alpha'\rangle\ . \qquad \text{(A1)}\end{aligned}$$

The partial wave state used in relativistic calculations $|\mathbf{P},k,q,\alpha\rangle$ corresponding to the total three-nucleon center of momentum, $\mathbf{P}=\mathbf{0}$, is given by [11]

$$\begin{aligned}|\mathbf{P},k,q,\alpha\rangle \;=\; |\mathbf{P},k,q(ls)j(\lambda\frac12)I(jI)JM;(t\frac12)T\rangle = \sum_{\mu_1\mu_2\mu_3}\sum_{\mu_2'\mu_3'}\sum_{\mu_s\mu_l\mu_\lambda\mu_I}\int d\hat{\mathbf{q}}\int d\hat{\mathbf{k}}Y_{l\mu_l}(\hat{\mathbf{k}})N(\mathbf{q}_2,\mathbf{q}_3) \\ (\frac12\frac12,s|\mu_2,\mu_3,\mu_s)(l,s,j|\mu_l,\mu_s,\mu) \\ D^{1/2}_{\mu_2'\mu_2}(R_{wc}(B_c(-q),k_2(\mathbf{q}_2,\mathbf{q}_3))D^{1/2}_{\mu_3'\mu_3}(R_{wc}(B_c(-q),k_3(\mathbf{q}_2,\mathbf{q}_3)) \\ Y_{\lambda\mu_\lambda}(\hat{\mathbf{q}})(\lambda,\frac12,I|\mu_\lambda,\mu_1,\mu_I)(j,I,J|\mu,\mu_I,M) \\ |\mathbf{q}+\frac13\mathbf{P},\mu_1\rangle|\mathbf{q}_2(\mathbf{k},-\mathbf{q})+\frac13\mathbf{P},\mu_2'\rangle|\mathbf{q}_3(-\mathbf{k},-\mathbf{q})+\frac13\mathbf{P},\mu_3'\rangle|(t,\frac12),T\rangle \qquad \text{(A2)}\end{aligned}$$

where

$$N^2(\mathbf{q}_2,\mathbf{q}_3) \;\equiv\; \mid\frac{\partial(\mathbf{q}_2\ \mathbf{q}_3)}{\partial(\mathbf{P}_{NN}\ \mathbf{k})}\mid = \frac{\bar M_0}{\omega_{\bar M_0}(P_{NN})}\ \frac{\omega_{q_2}}{\omega_k}\ \frac{\omega_{q_3}}{\omega_k} \qquad \text{(A3)}$$

is the Jacobian for the Lorentz transformation from $(\mathbf{q}_2,\mathbf{q}_3)$ to $(\mathbf{P}_{NN},\mathbf{k}) = (-\mathbf{q},\mathbf{k})$, $\omega_k = \sqrt{m^2+k^2}$, $\bar M_0 = 2\omega_k = \omega_{q_2}+\omega_{q_3}$, and $\omega_{\bar M_0}(P_{NN}) = \sqrt{\bar M_0^2+P_{NN}^2}$. The momentum $\mathbf{k}_2(\mathbf{q}_2,\mathbf{q}_3)=\mathbf{k}$ and $\mathbf{k}_3(\mathbf{q}_2,\mathbf{q}_3) = -\mathbf{k}_2(\mathbf{q}_2,\mathbf{q}_3)$.

The nonrelativistic partial-wave state $|\mathbf{P}',\tilde p,\tilde q,\tilde\alpha\rangle$ with standard Jacobi momenta is given by

$$|\mathbf{P}',\tilde p,\tilde q,\tilde\alpha\rangle \;=\; \sum_{\tilde\nu_1,\tilde\nu_2,\tilde\nu_3}\sum_{\tilde\nu_s,\tilde\nu_l,\tilde\nu_\lambda,\tilde\nu_I}\int d\hat{\tilde{\mathbf{p}}}\int d\hat{\tilde{\mathbf{q}}}Y_{\tilde l\tilde\nu_l}(\hat{\tilde{\mathbf{p}}})Y_{\tilde\lambda\tilde\nu_\lambda}(\hat{\tilde{\mathbf{q}}})$$

$$(\frac{1}{2},\frac{1}{2},\tilde{s}|\tilde{\nu}_2,\tilde{\nu}_3,\tilde{\nu}_s)(\tilde{l},\tilde{s},\tilde{j}|\tilde{\nu}_l,\tilde{\nu}_s,\tilde{\nu})(\tilde{\lambda},\frac{1}{2},\tilde{I}|\tilde{\nu}_\lambda,\tilde{\nu}_1,\tilde{\nu}_I)(\tilde{j},\tilde{I},\tilde{J}|\tilde{\nu},\tilde{\nu}_I,\tilde{M})$$
$$|\tilde{\mathbf{q}}+\frac{1}{3}\mathbf{P}',\tilde{\nu}_1\rangle|\tilde{\mathbf{q}}_2^{nr}+\frac{1}{3}\mathbf{P}',\tilde{\nu}_2\rangle|\tilde{\mathbf{q}}_3^{nr}+\frac{1}{3}\mathbf{P}',\tilde{\nu}_3\rangle|(\tilde{t}\frac{1}{2})\tilde{T}\rangle \tag{A4}$$

where in the three-nucleon center of momentum system the nonrelativistic momenta $\tilde{\mathbf{q}}_2{}^{nr}$ and $\tilde{\mathbf{q}}_3{}^{nr}$ of the nucleons 2 and 3 are given by standard Jacobi momenta $\tilde{\mathbf{p}}$ and $\tilde{\mathbf{q}}$ as

$$\begin{aligned}\tilde{\mathbf{q}}_2{}^{nr} &= \tilde{\mathbf{p}}-\frac{\tilde{\mathbf{q}}}{2}\\ \tilde{\mathbf{q}}_3{}^{nr} &= -\tilde{\mathbf{p}}-\frac{\tilde{\mathbf{q}}}{2}\ .\end{aligned} \tag{A5}$$

That leads to the scalar product $\langle \mathbf{P},k,q,\alpha|\mathbf{P}',\tilde{p},\tilde{q},\tilde{\alpha}\rangle$

$$\begin{aligned}\langle \mathbf{P},k,q,\alpha\ |\ \mathbf{P}',\tilde{p},\tilde{q},\tilde{\alpha}\rangle = &\sum_{\mu_1\mu_2\mu_3}\sum_{\mu_2'\mu_3'}\sum_{\mu_s\mu_l\mu_\lambda\mu_I}\int d\hat{\mathbf{q}}\int d\hat{\mathbf{k}}Y^*_{l\mu_l}(\hat{\mathbf{k}})N(\mathbf{q}_2,\mathbf{q}_3)\\
&(\frac{1}{2},\frac{1}{2},s|\mu_2,\mu_3,\mu_s)(l,s,j|\mu_l,\mu_s,\mu)\\
&D^{1/2*}_{\mu_2'\mu_2}(R_{wc}(B_c(-q),k_2(\mathbf{q}_2,\mathbf{q}_3))D^{1/2*}_{\mu_3'\mu_3}(R_{wc}(B_c(-q),k_3(\mathbf{q}_2,\mathbf{q}_3))\\
&Y^*_{\lambda\mu_\lambda}(\hat{\mathbf{q}})(\lambda,\frac{1}{2},I|\mu_\lambda,\mu_1,\mu_I)(j,I,J|\mu,\mu_I,M)\\
&\sum_{\tilde{\nu}_s\tilde{\nu}_l\tilde{\nu}_\lambda\tilde{\nu}_I}\int d\hat{\tilde{\mathbf{p}}}\int d\hat{\tilde{\mathbf{q}}}Y_{\tilde{l}\tilde{\nu}_l}(\hat{\tilde{\mathbf{p}}})Y_{\tilde{\lambda},\tilde{\nu}_\lambda}(\hat{\tilde{\mathbf{q}}})(\frac{1}{2},\frac{1}{2},\tilde{s}|\mu_2',\mu_3',\tilde{\nu}_s)(\tilde{l},\tilde{s},\tilde{j}|\tilde{\nu}_l,\tilde{\nu}_s,\tilde{\nu})\\
&(\tilde{\lambda},\frac{1}{2},\tilde{I}|\tilde{\nu}_\lambda,\mu_1,\tilde{\nu}_I)(\tilde{j},\tilde{I}\tilde{J}|\tilde{\nu},\tilde{\nu}_I,\tilde{M})\\
&\delta(\mathbf{q}-\tilde{\mathbf{q}}+\frac{1}{3}(\mathbf{P}-\mathbf{P}'))\delta(\mathbf{q}_2(\mathbf{k},-\mathbf{q})-\tilde{\mathbf{q}}_2{}^{nr}+\frac{1}{3}(\mathbf{P}-\mathbf{P}'))\\
&\delta(\mathbf{q}_3(-\mathbf{k},-\mathbf{q})-\tilde{\mathbf{q}}_3{}^{nr}+\frac{1}{3}(\mathbf{P}-\mathbf{P}'))\left\langle(t\frac{1}{2})T|(\tilde{t}\frac{1}{2})\tilde{T}\right\rangle\ .\end{aligned} \tag{A6}$$

That matrix element should be proportional to $\delta_{J\tilde{J}}\delta_{M\tilde{M}}$ and independent from M. Thus

$$\begin{aligned}\langle \mathbf{P},k,q,\alpha\ |\ \mathbf{P}',\tilde{p},\tilde{q},\tilde{\alpha}\rangle = &\frac{1}{2J+1}\sum_M\sum_{\mu_1,\mu_2,\mu_3}\sum_{\mu_2'\mu_3'}\sum_{\mu_s,\mu_l,\mu_\lambda,\mu_I}\int d\hat{\mathbf{q}}\int d\hat{\mathbf{k}}Y^*_{l\mu_l}(\hat{\mathbf{k}})N(\mathbf{q}_2,\mathbf{q}_3)\\
&(\frac{1}{2},\frac{1}{2},s|\mu_2,\mu_3,\mu_s)(l,s,j|\mu_l,\mu_s,\mu)\\
&D^{1/2*}_{\mu_2'\mu_2}(R_{wc}(B_c(-q),k_2(\mathbf{q}_2,\mathbf{q}_3))D^{1/2*}_{\mu_3'\mu_3}(R_{wc}(B_c(-q),k_3(\mathbf{q}_2,\mathbf{q}_3))\\
&Y^*_{\lambda\mu_\lambda}(\hat{\mathbf{q}})(\lambda,\frac{1}{2},I|\mu_\lambda,\mu_1,\mu_I)(j,I,J|\mu,\mu_I,M)\\
&\sum_{\tilde{\nu}_s\tilde{\nu}_l\tilde{\nu}_\lambda\tilde{\nu}_I}\int d\hat{\tilde{\mathbf{p}}}\int d\hat{\tilde{\mathbf{q}}}Y_{\tilde{l}\tilde{\nu}_l}(\hat{\tilde{\mathbf{p}}})Y_{\tilde{\lambda}\tilde{\nu}_\lambda}(\hat{\tilde{\mathbf{q}}})(\frac{1}{2},\frac{1}{2},\tilde{s}|\mu_2',\mu_3',\tilde{\nu}_s)(\tilde{l},\tilde{s},\tilde{j}|\tilde{\nu}_l,\tilde{\nu}_s,\tilde{\nu})\\
&(\tilde{\lambda},\frac{1}{2},\tilde{I}|\tilde{\nu}_\lambda,\mu_1,\tilde{\nu}_I)(\tilde{j},\tilde{I},J|\tilde{\nu},\tilde{\nu}_I,M)\\
&\delta(\mathbf{q}-\tilde{\mathbf{q}}+\frac{1}{3}(\mathbf{P}-\mathbf{P}'))\delta(\mathbf{q}_2(\mathbf{k},-\mathbf{q})-\tilde{\mathbf{q}}_2{}^{nr}+\frac{1}{3}(\mathbf{P}-\mathbf{P}'))\\
&\delta(\mathbf{q}_3(-\mathbf{k},-\mathbf{q})-\tilde{\mathbf{q}}_3{}^{nr}+\frac{1}{3}(\mathbf{P}-\mathbf{P}'))\langle(t\frac{1}{2}T)|(\tilde{t}\frac{1}{2})\tilde{T}\rangle\ .\end{aligned} \tag{A7}$$

The momenta of nucleons 2 and 3 in the three-nucleon center of momentum system are given through their two-nucleon center of momentum relative momentum $\mathbf{k}$ and the momentum of the

spectator nucleon 1, $\mathbf{q}$, by

$$\mathbf{q}_2(\mathbf{k},-\mathbf{q}) \;=\; \mathbf{k}-\frac{\mathbf{q}}{2}+\frac{\mathbf{k}\cdot\mathbf{q}}{2\omega_k(2\omega_k+\bar{M}_0)}\mathbf{q} \tag{A8}$$

and

$$\mathbf{q}_3(-\mathbf{k},-\mathbf{q}) \;=\; -\mathbf{k}-\frac{\mathbf{q}}{2}-\frac{\mathbf{k}\cdot\mathbf{q}}{2\omega_k(2\omega_k+\bar{M}_0)}\mathbf{q}\;. \tag{A9}$$

That allows to write the three δ-functions in the form

$$\begin{aligned}
&\delta(\mathbf{q}-\tilde{\mathbf{q}}+\frac{1}{3}(\mathbf{P}-\mathbf{P}'))\delta(\mathbf{q}_2(\mathbf{k},-\mathbf{q})-{\tilde{\mathbf{q}}_2}^{nr}+\frac{1}{3}(\mathbf{P}-\mathbf{P}'))\delta(\mathbf{q}_3(-\mathbf{k},-\mathbf{q})-{\tilde{\mathbf{q}}_3}^{nr}+\frac{1}{3}(\mathbf{P}-\mathbf{P}'))=\\
&\delta(\mathbf{q}-\tilde{\mathbf{q}}+\frac{1}{3}(\mathbf{P}-\mathbf{P}'))\delta(-\tilde{\mathbf{p}}+\mathbf{k}+\frac{\mathbf{k}\cdot\mathbf{q}}{2\omega_k(2\omega_k+\bar{M}_0)}\mathbf{q}+\frac{1}{3}(\mathbf{P}-\mathbf{P}'))\\
&\delta(\tilde{\mathbf{p}}-\mathbf{k}-\frac{\mathbf{k}\cdot\mathbf{q}}{2\omega_k(2\omega_k+\bar{M}_0)}\mathbf{q}+\frac{1}{3}(\mathbf{P}-\mathbf{P}'))=\\
&\delta(\mathbf{q}-\tilde{\mathbf{q}})\delta(\tilde{\mathbf{p}}-\mathbf{k}-\frac{\mathbf{k}\cdot\mathbf{q}}{2\omega_k(2\omega_k+\bar{M}_0)}\mathbf{q})\delta(\mathbf{P}-\mathbf{P}')\;.
\end{aligned} \tag{A10}$$

In the following we assume the three-nucleon center of momentum system ($\mathbf{P}=\mathbf{P}'=\mathbf{0}$) and drop the $\delta(\mathbf{P}-\mathbf{P}')$ in all expressions. Performing the integration over $d\hat{\tilde{\mathbf{q}}}$ one gets

$$\begin{aligned}
\langle k,q,\alpha|\tilde{p},\tilde{q},\tilde{\alpha}\rangle \;=\; &\frac{1}{2J+1}\sum_M\sum_{\mu_1\mu_2\mu_3}\sum_{\mu_2'\mu_3'}\sum_{\mu_s\mu_l\mu_\lambda\mu_I}\frac{\delta(q-\tilde{q})}{q\tilde{q}}\int d\hat{\mathbf{q}}\int d\hat{\mathbf{k}}\int d\hat{\tilde{\mathbf{p}}}\,Y^*_{l\mu_l}(\hat{\mathbf{k}})\\
&N(\mathbf{q}_2,\mathbf{q}_3)(\frac{1}{2},\frac{1}{2},s|\mu_2,\mu_3,\mu_s)(l,s,j|\mu_l,\mu_s,\mu)\\
&D^{1/2*}_{\mu_2'\mu_2}(R_{wc}(B_c(-q),k_2(\mathbf{q}_2,\mathbf{q}_3))D^{1/2*}_{\mu_3'\mu_3}(R_{wc}(B_c(-q),k_3(\mathbf{q}_2,\mathbf{q}_3))\\
&Y^*_{\lambda\mu_\lambda}(\hat{\mathbf{q}})(\lambda,\frac{1}{2},I|\mu_\lambda,\mu_1,\mu_I)(j,I,J|\mu,\mu_I,M)\sum_{\tilde{\nu}_s,\tilde{\nu}_l,\tilde{\nu}_\lambda,\tilde{\nu}_I}Y_{\tilde{l}\tilde{\nu}_l}(\hat{\tilde{\mathbf{p}}})Y_{\tilde{\lambda}\tilde{\nu}_\lambda}(\hat{\mathbf{q}})\\
&(\frac{1}{2},\frac{1}{2},\tilde{s}|\mu_2',\mu_3',\tilde{\nu}_s)(\tilde{l},\tilde{s},\tilde{j}|\tilde{\nu}_l,\tilde{\nu}_s,\tilde{\nu})(\tilde{\lambda},\frac{1}{2},\tilde{I}|\tilde{\nu}_\lambda,\mu_1,\tilde{\nu}_I)(\tilde{j},\tilde{I},J|\tilde{\nu},\tilde{\nu}_I,M)\\
&\delta(\tilde{\mathbf{p}}-\mathbf{k}-\frac{\mathbf{k}\cdot\mathbf{q}}{2\omega_k(2\omega_k+\bar{M}_0)}\mathbf{q})\langle(t\frac{1}{2})T|(\tilde{t}\frac{1}{2})\tilde{T}\rangle\;.
\end{aligned} \tag{A11}$$

That matrix element is a scalar which depends on the angles between the vectors $\mathbf{q}$, $\mathbf{k}$ and $\tilde{\mathbf{p}}$. These angles are fixed by the δ-function $\delta(\tilde{\mathbf{p}}-\mathbf{k}-\frac{\mathbf{k}\cdot\mathbf{q}}{2\omega_k(2\omega_k+\bar{M}_0)}\mathbf{q})$. Namely, while $\tilde{\mathbf{p}}=\mathbf{k}+\frac{\mathbf{k}\cdot\mathbf{q}}{2\omega_k(2\omega_k+\bar{M}_0)}\mathbf{q}$ it follows that

$$\begin{aligned}
\mathbf{k}\cdot\tilde{\mathbf{p}} \;&=\; \mathbf{k}\cdot\mathbf{k}+\frac{(\mathbf{k}\cdot\mathbf{q})^2}{2\omega_k(2\omega_k+\bar{M}_0)}\;,\\
\mathbf{q}\cdot\tilde{\mathbf{p}} \;&=\; \mathbf{q}\cdot\mathbf{k}+\frac{(\mathbf{q}\cdot\mathbf{q})(\mathbf{k}\cdot\mathbf{q})}{2\omega_k(2\omega_k+\bar{M}_0)}\;,\\
\tilde{\mathbf{p}}\cdot\tilde{\mathbf{p}} \;&=\; \tilde{\mathbf{p}}\cdot\mathbf{k}+\frac{(\tilde{\mathbf{p}}\cdot\mathbf{q})(\mathbf{k}\cdot\mathbf{q})}{2\omega_k(2\omega_k+\bar{M}_0)}\;.
\end{aligned} \tag{A12}$$

Therefore one can take $\hat{\mathbf{q}}$ pointing in z-direction, what for given k, q, and $\tilde{p}$ values, defines all angles between the appearing vectors. That allows to perform the integration over $d\hat{\mathbf{q}}$ resulting in

$$\langle k,q,\alpha|\tilde{p},\tilde{q},\tilde{\alpha}\rangle \;=\; \frac{8\pi^2}{2J+1}\int_{-1}^{+1}dx\frac{\delta(q-\tilde{q})}{q\tilde{q}}\frac{\delta(\tilde{p}-|\mathbf{k}+\frac{\mathbf{k}\cdot\mathbf{q}}{2\omega_k(2\omega_k+\bar{M}_0)}\mathbf{q}|)}{\tilde{p}^2}\sum_M\sum_{\mu_1\mu_2\mu_3}\sum_{\mu_2'\mu_3'}\sum_{\mu_s\mu_l\mu_\lambda\mu_I}Y^*_{l\mu_l}(\hat{\mathbf{k}})$$

$$
\begin{aligned}
&N(\mathbf{q}_2,\mathbf{q}_3)(\frac{1}{2},\frac{1}{2},s|\mu_2,\mu_3,\mu_s)(l,s,j|\mu_l,\mu_s,\mu)\\
&D^{1/2*}_{\mu_2'\mu_2}(R_{wc}(B_c(-q),k_2(\mathbf{q}_2,\mathbf{q}_3))D^{1/2*}_{\mu_3'\mu_3}(R_{wc}(B_c(-q),k_3(\mathbf{q}_2,\mathbf{q}_3))\\
&Y^*_{\lambda\mu_\lambda}(\hat{\mathbf{q}})(\lambda,\frac{1}{2},I|\mu_\lambda,\mu_1,\mu_I)(j,I,J|\mu,\mu_I,M)\sum_{\tilde\nu_s\tilde\nu_l\tilde\nu_\lambda\tilde\nu_I}Y_{\tilde l\tilde\nu_l}(\hat{\tilde{\mathbf{p}}})Y_{\tilde\lambda\tilde\nu_\lambda}(\hat{\mathbf{q}})\\
&(\frac{1}{2},\frac{1}{2},\tilde s|\mu_2',\mu_3',\tilde\nu_s)(\tilde l,\tilde s,\tilde j|\tilde\nu_l,\tilde\nu_s,\tilde\nu)(\tilde\lambda,\frac{1}{2},\tilde I|\tilde\nu_\lambda,\mu_1,\tilde\nu_I)\\
&(\tilde j,\tilde I,J|\tilde\nu,\tilde\nu_I,M)\langle(t,\frac{1}{2}),T|(\tilde t,\frac{1}{2}),\tilde T\rangle
\end{aligned}
\tag{A13}
$$

with $x\equiv\hat{\mathbf{q}}\cdot\hat{\mathbf{k}}$. We have chosen the coordinate system with $\mathbf{q}$ parallel to the z axis which leads to the components of $\mathbf{q}$, $\mathbf{k}$, $\tilde{\mathbf{p}}$

$$
\begin{aligned}
\mathbf{q} &= (0,0,q)\ ,\\
\mathbf{k} &= (k\sqrt{1-x^2},0,kx)\ ,\\
\tilde{\mathbf{p}} &= (k\sqrt{1-x^2},0,kx(1+\frac{q^2}{2\omega_k(2\omega_k+\bar M_0)}))\ .
\end{aligned}
\tag{A14}
$$

The isospin factor is

$$
\left\langle(t,\frac{1}{2}),T|(\tilde t,\frac{1}{2}),\tilde T\right\rangle = \delta_{t\tilde t}\delta_{T\tilde T}\delta_{M_TM_{\tilde T}}\delta_{\nu_t\nu_{\tilde t}}\ .
\tag{A15}
$$

Taking that all together gives

$$
\begin{aligned}
\langle k,q,\alpha|\tilde p,\tilde q,\tilde\alpha\rangle &= \delta_{t\tilde t}\delta_{T\tilde T}\frac{2\pi\sqrt{(2\lambda+1)(2\tilde\lambda+1)}}{2J+1}\int_{-1}^{+1}dx\frac{\delta(q-\tilde q)}{q\tilde q}\frac{\delta(\tilde p-|\mathbf{k}+\frac{\mathbf{k}\cdot\mathbf{q}}{2\omega_k(2\omega_k+M_0)}\mathbf{q}|)}{\tilde p^2}\\
&\sum_M\sum_{\mu_1\mu_2\mu_3}\sum_{\mu_2'\mu_3'}Y^*_{l,M-\mu_1-\mu_2-\mu_3}(\hat{\mathbf{k}})N(\mathbf{q}_2,\mathbf{q}_3)\\
&D^{1/2*}_{\mu_2'\mu_2}(R_{wc}(B_c(-q),k_2(\mathbf{q}_2,\mathbf{q}_3))D^{1/2*}_{\mu_3'\mu_3}(R_{wc}(B_c(-q),-k_3(\mathbf{q}_2,\mathbf{q}_3))\\
&(\frac{1}{2},\frac{1}{2},s|\mu_2,\mu_3,\mu_2+\mu_3)(lsj|M-\mu_l-\mu_2-\mu_3,\mu_2+\mu_3,M-\mu_1)\\
&(\lambda,\frac{1}{2},I|0,\mu_1,\mu_1)(j,I,J|M-\mu_1,\mu_1,M)Y_{\tilde l,M-\mu_1-\mu_2'-\mu_3'}(\hat{\tilde{\mathbf{p}}})\\
&(\frac{1}{2},\frac{1}{2},\tilde s|\mu_2',\mu_3',\mu_2'+\mu_3')(\tilde l,\tilde s,\tilde j|M-\mu_1-\mu_2'-\mu_3',\mu_2'+\mu_3',M-\mu_1)\\
&(\tilde\lambda,\frac{1}{2},\tilde I|0,\mu_1\mu_1)(\tilde j,\tilde I,J|M-\mu_1,\mu_1,M)\ .
\end{aligned}
\tag{A16}
$$

The resulting expression for the matrix element $\langle k,q,\alpha|\,V_4^{(1)}(1+P)\,|k,'\,q',\alpha'\rangle$ is given by

$$
\begin{aligned}
&\langle k,q,\alpha|V_4^{(1)}(1+P)|k',q',\alpha'\rangle=\sum_{\tilde\alpha}\delta_{t\tilde t}\delta_{T\tilde T}\frac{2\pi\sqrt{(2\lambda+1)(2\tilde\lambda+1)}}{2J+1}\\
&\int_{-1}^{+1}dx\sum_M\sum_{\mu_1\mu_2\mu_3}\sum_{\bar\mu_2\bar\mu_3}Y^*_{l,M-\mu_1-\mu_2-\mu_3}(\hat{\mathbf{k}})N(\mathbf{q}_2,\mathbf{q}_3)\\
&D^{1/2*}_{\bar\mu_2\mu_2}(R_{wc}(B_c(-q),k_2(\mathbf{q}_2,\mathbf{q}_3))D^{1/2*}_{\bar\mu_3\mu_3}(R_{wc}(B_c(-q),k_3(\mathbf{q}_2,\mathbf{q}_3))\\
&(\frac{1}{2},\frac{1}{2},s|\mu_2,\mu_3,\mu_2+\mu_3)(l,s,j|M-\mu_l-\mu_2-\mu_3,\mu_2+\mu_3,M-\mu_1)
\end{aligned}
$$

$$
\begin{aligned}
&(\lambda,\frac{1}{2},I|0,\mu_1,\mu_1)(j,I,J|M-\mu_1,\mu_1,M)Y_{\tilde{l},M-\mu_1-\bar{\mu}_2-\bar{\mu}_3}(\hat{\tilde{\mathbf{p}}})\\
&(\frac{1}{2},\frac{1}{2},\tilde{s}|\bar{\mu}_2,\bar{\mu}_3,\bar{\mu}_2+\bar{\mu}_3)(\tilde{l},\tilde{s},\tilde{j}|M-\mu_1-\bar{\mu}_2-\bar{\mu}_3,\bar{\mu}_2+\bar{\mu}_3,M-\mu_1)\\
&(\tilde{\lambda},\frac{1}{2},\tilde{I}|0,\mu_1,\mu_1)(\tilde{j},\tilde{I},J|M-\mu_1,\mu_1,M)\sum_{\tilde{\alpha}'}\delta_{t't'}\delta_{T'\tilde{T}'}\frac{2\pi\sqrt{(2\lambda'+1)(2\tilde{\lambda}'+1)}}{2J+1}\\
&\int_{-1}^{+1}dx'\sum_{M}\sum_{\mu_1'\mu_2'\mu_3'}\sum_{\bar{\mu}_2'\bar{\mu}_3'}Y_{l',M-\mu_1'-\mu_2'-\mu_3'}(\hat{\mathbf{k}}')N(\mathbf{q}_2',\mathbf{q}_3')\\
&D^{1/2}_{\bar{\mu}_2'\mu_2'}(R_{wc}(B_c(-q'),k_2'(\mathbf{q}_2',\mathbf{q}_3'))D^{1/2}_{\bar{\mu}_3'\mu_3'}(R_{wc}(B_c(-q'),k_3'(\mathbf{q}_2',\mathbf{q}_3'))\\
&(\frac{1}{2},\frac{1}{2},s'|\mu_2',\mu_3',\mu_2'+\mu_3')(l',s',j'|M-\mu_l'-\mu_2'-\mu_3',\mu_2'+\mu_3',M-\mu_1')\\
&(\lambda',\frac{1}{2},I'|0,\mu_1',\mu_1')(j',I',J|M-\mu_1',\mu_1',M)Y_{\tilde{l}',M-\mu_1'-\bar{\mu}_2'-\bar{\mu}_3'}(\hat{\tilde{\mathbf{p}}}')\\
&(\frac{1}{2},\frac{1}{2},\tilde{s}'|\bar{\mu}_2',\bar{\mu}_3',\bar{\mu}_2'+\bar{\mu}_3')(\tilde{l}',\tilde{s}',\tilde{j}'|M-\mu_1'-\bar{\mu}_2'-\bar{\mu}_3',\bar{\mu}_2'+\bar{\mu}_3',M-\mu_1')\\
&(\tilde{\lambda}',\frac{1}{2},\tilde{I}'|0,\mu_1',\mu_1')(\tilde{j}',\tilde{I}',J|M-\mu_1',\mu_1',M)\\
&\langle|\mathbf{k}+\frac{\mathbf{k}\cdot\mathbf{q}}{2\omega_k(2\omega_k+\bar{M}_0)}\mathbf{q}\;|,q,\alpha|V_4^{(1)}(1+P)||\mathbf{k}'+\frac{\mathbf{k}'\cdot\mathbf{q}'}{2\omega_{k'}(2\omega_{k'}+\bar{M}_0)}\mathbf{q}'|,q',\tilde{\alpha}'\rangle\ .
\end{aligned}
\tag{A17}
$$

Appendix B: Transformation of a 3-dimensional three-nucleon force matrix element from $(\mathbf{p},\mathbf{q})$ to $(\mathbf{k},\mathbf{q})$ momenta

We would like to express directly the matrix element $\langle\mathbf{k},\mathbf{q}\,|\,V_4^{(1)}\,|\mathbf{k}',\mathbf{q}'\rangle$ by that matrix element given in terms of single-nucleon momenta $\langle\mathbf{q}_1,\mathbf{q}_2,\mathbf{q}_3|\,V_4^{(1)}\,|\mathbf{q}_1',\mathbf{q}_2',\mathbf{q}_3'\rangle$. For momenta $\mathbf{q}_2$ and $\mathbf{q}_3$ of nucleons 2 and 3 in three-nucleon center of momentum system their relative momentum $\mathbf{k}(\mathbf{q}_2,\mathbf{q}_3)$ in the two-nucleon center of momentum subsystem of nucleons 2 and 3 is

$$
\mathbf{k}(\mathbf{q}_2,\mathbf{q}_3)=\frac{1}{2}[\mathbf{q}_2-\mathbf{q}_3-(\mathbf{q}_2+\mathbf{q}_3)\frac{E_2-E_3}{E_2+E_3+\sqrt{(E_2+E_3)^2-(\mathbf{q}_2+\mathbf{q}_3)^2}}] \tag{B1}
$$

with $E_i=\sqrt{m^2+{q_i}^2}$.

Using completeness of $|\mathbf{q}_1\mathbf{q}_2\mathbf{q}_3\rangle$ states one gets

$$
\begin{aligned}
\langle\mathbf{k},\mathbf{q}|V_4^{(1)}|\mathbf{k}',\mathbf{q}'\rangle\ &=\ \int d\mathbf{q}_1d\mathbf{q}_2d\mathbf{q}_3\delta(\mathbf{q}_1+\mathbf{q}_2+\mathbf{q}_3)\langle\mathbf{k},\mathbf{q}|\mathbf{q}_1,\mathbf{q}_2,\mathbf{q}_3\rangle\langle\mathbf{q}_1,\mathbf{q}_2,\mathbf{q}_3|V_4^{(1)}\\
&\quad\int d\mathbf{q}_1'd\mathbf{q}_2'd\mathbf{q}_3'|\mathbf{q}_1'\mathbf{q}_2'\mathbf{q}_3'\rangle\langle\mathbf{q}_1',\mathbf{q}_2',\mathbf{q}_3'|\mathbf{k}',\mathbf{q}'\rangle\delta(\mathbf{q}_1'+\mathbf{q}_2'+\mathbf{q}_3')\\
&=\ \int d\mathbf{q}_1d\mathbf{q}_2d\mathbf{q}_3\delta(\mathbf{q}_1+\mathbf{q}_2+\mathbf{q}_3)\delta(\mathbf{q}-\mathbf{q}_1)\delta(\mathbf{k}-\mathbf{k}(\mathbf{q}_2,\mathbf{q}_3))\\
&\quad\int d\mathbf{q}_1'd\mathbf{q}_2'd\mathbf{q}_3'\delta(\mathbf{q}_1'+\mathbf{q}_2'+\mathbf{q}_3')\delta(\mathbf{q}'-\mathbf{q}_1')\delta(\mathbf{k}'-\mathbf{k}'(\mathbf{q}_2',\mathbf{q}_3'))\\
&\quad\frac{1}{N(\mathbf{q}_2,\mathbf{q}_3)}\frac{1}{N(\mathbf{q}_2',\mathbf{q}_3')}\langle\mathbf{q}_1\mathbf{q}_2\mathbf{q}_3|V_4^{(1)}|\mathbf{q}_1'\mathbf{q}_2'\mathbf{q}_3'\rangle\\
&\quad=\int d\mathbf{q}_2d\mathbf{q}_3\delta(\mathbf{q}+\mathbf{q}_2+\mathbf{q}_3)\delta(\mathbf{k}-\mathbf{k}(\mathbf{q}_2,\mathbf{q}_3))\\
&\quad\int d\mathbf{q}_2'd\mathbf{q}_3'\delta(\mathbf{q}'+\mathbf{q}_2'+\mathbf{q}_3')\delta(\mathbf{k}'-\mathbf{k}'(\mathbf{q}_2',\mathbf{q}_3'))
\end{aligned}
$$

$$
\begin{aligned}
&\frac{1}{N(\mathbf{q}_2,\mathbf{q}_3)}\frac{1}{N(\mathbf{q}_2',\mathbf{q}_3')}\langle \mathbf{q},\mathbf{q}_2,\mathbf{q}_3|V_4^{(1)}|\mathbf{q}',\mathbf{q}_2',\mathbf{q}_3'\rangle \\
&= \int d\mathbf{k}(\mathbf{q}_2,\mathbf{q}_3)d(\mathbf{q}_2+\mathbf{q}_3)\delta(\mathbf{q}+\mathbf{q}_2+\mathbf{q}_3)\delta(\mathbf{k}-\mathbf{k}(\mathbf{q}_2,\mathbf{q}_3)) \\
&\int d\mathbf{k}'(\mathbf{q}_2',\mathbf{q}_3')d(\mathbf{q}_2'+\mathbf{q}_3')\delta(\mathbf{q}'+\mathbf{q}_2'+\mathbf{q}_3')\delta(\mathbf{k}'-\mathbf{k}'(\mathbf{q}_2',\mathbf{q}_3')) \\
&N(\mathbf{q}_2,\mathbf{q}_3)N(\mathbf{q}_2',\mathbf{q}_3')\langle \mathbf{q},\mathbf{q}_2,\mathbf{q}_3|V_4^{(1)}|\mathbf{q}',\mathbf{q}_2',\mathbf{q}_3'\rangle \ . \qquad \text{(B2)}
\end{aligned}
$$

For given vectors $\mathbf{k}(\mathbf{q}_2,\mathbf{q}_3)=\mathbf{k}_0$ and $\mathbf{q}_2+\mathbf{q}_3=-\mathbf{q}_0$ the vectors $\mathbf{q}_2$ and $\mathbf{q}_3$ are given by: $\mathbf{q}_2=-\mathbf{q}_0-\mathbf{q}_3^0$ and $\mathbf{q}_3=\mathbf{q}_3^0$ with $\mathbf{q}_3^0$ being the solution of the equation

$$
\mathbf{k}_0-\mathbf{k}(-\mathbf{q}_0-\mathbf{q}_3^0,\mathbf{q}_3^0)=\mathbf{0} \qquad \text{(B3)}
$$

and similarily for the primed quantities.

Thus one gets

$$
\begin{aligned}
\langle \mathbf{kq}|\, V_4^{(1)}\,|\mathbf{k}'\mathbf{q}'\rangle \ &= \ N(-\mathbf{q}-\mathbf{q}_3^0,\mathbf{q}_3^0)N(-\mathbf{q}'-\mathbf{q}_3^{0\prime},\mathbf{q}_3^{0\prime}) \\
&\quad \left\langle \mathbf{q},-\mathbf{q}-\mathbf{q}_3^0,\mathbf{q}_3^0\right| V_4^{(1)}\left|\mathbf{q}',-\mathbf{q}'-\mathbf{q}_3^{0\prime},\mathbf{q}_3^{0\prime}\right\rangle \\
&= \ N(-\mathbf{q}-\mathbf{q}_3^0,\mathbf{q}_3^0)N(-\mathbf{q}'-\mathbf{q}_3^{0\prime},\mathbf{q}_3^{0\prime}) \\
&\quad \left\langle \mathbf{p}=-\frac{1}{2}\mathbf{q}-\mathbf{q}_3^0,\mathbf{q}\right| V_4^{(1)}\left|\mathbf{p}'=-\frac{1}{2}\mathbf{q}'-\mathbf{q}_3^{0\prime},\mathbf{q}'\right\rangle \ . \qquad \text{(B4)}
\end{aligned}
$$

Starting from (44) and following the same steps as in (B2) one gets for the partial wave projected matrix elements

$$
\begin{aligned}
\langle k,q,\alpha|V_4^{(1)}|k',q',\alpha'\rangle \ &= \ \int d\hat{\mathbf{k}}d\hat{\mathbf{q}}_1 \sum_{\bar{\mu}_2\bar{\mu}_3}\sum_{\mu_2\mu_3\mu_s}\sum_{\mu_l\mu_\lambda\mu_I}(\frac{1}{2},\mu_2,\frac{1}{2},\mu_3|s,\mu_s)(l,\mu_l,s,\mu_s,|j,\mu_j) \\
&(\lambda,\mu_\lambda,\frac{1}{2},\mu_1|I,\mu_I)(j,\mu_j,I,\mu_I|J,\mu)\ Y^*_{\lambda\mu_\lambda}(\hat{\mathbf{q}}_1)Y^*_{l\mu_l}(\hat{\mathbf{k}}) \\
&D^{\frac{1}{2}*}_{\bar{\mu}_2\mu_2}[R_{wc}(\ B_c(-q_1),k_2(\ \mathbf{q}_2,\mathbf{q}_3)\ )] \\
&D^{\frac{1}{2}*}_{\bar{\mu}_3\mu_3}[R_{wc}(\ B_c(-q_1),k_3(\ \mathbf{q}_2,\mathbf{q}_3)\ )] \\
&\int d\hat{\mathbf{k}}'d\hat{\mathbf{q}}_1' \sum_{\bar{\mu}_2'\bar{\mu}_3'}\sum_{\mu_2'\mu_3'\mu_s'}\sum_{\mu_l'\mu_\lambda'\mu_I'}(\frac{1}{2},\mu_2',\frac{1}{2},\mu_3'|s',\mu_s')(l',\mu_l',s',\mu_s',|j',\mu_j') \\
&(\lambda',\mu_\lambda',\frac{1}{2},\mu_1'|I',\mu_I')(j',\mu_j',I',\mu_I'|J,\mu)Y_{\lambda'\mu_\lambda'}(\hat{\mathbf{q}}_1')Y_{l'\mu_l'}(\hat{\mathbf{k}}') \\
&D^{\frac{1}{2}}_{\bar{\mu}_2'\mu_2'}[R_{wc}(\ B_c(-q_1'),k_2'(\ \mathbf{q}_2',\mathbf{q}_3')\ )] \\
&D^{\frac{1}{2}}_{\bar{\mu}_3'\mu_3'}[R_{wc}(\ B_c(-q_1'),k_3(\ \mathbf{q}_2',\mathbf{q}_3')\ )] \\
&N(\mathbf{q}_2,\mathbf{q}_3)N(\mathbf{q}_2',\mathbf{q}_3')\langle \mathbf{q},\mathbf{q}_2,\mathbf{q}_3|V_4^{(1)}|\mathbf{q}',\mathbf{q}_2',\mathbf{q}_3'\rangle \ , \qquad \text{(B5)}
\end{aligned}
$$

where $\mathbf{q}_1\equiv q\hat{\mathbf{q}}_1$, $\mathbf{k}_2(\mathbf{q}_2,\mathbf{q}_3)\equiv k\hat{\mathbf{k}}$, $\mathbf{k}_3(\mathbf{q}_2,\mathbf{q}_3)=-\mathbf{k}_2(\mathbf{q}_2,\mathbf{q}_3)$, and $\mathbf{q}_2$ together with $\mathbf{q}_3$ result from (B3) and similarily for primed quantities. These partial wave matrix elements can be obtained using automatized partial wave expansion of Ref. [30].

[1] R.B. Wiringa, V.G.J. Stoks, R. Schiavilla, Phys. Rev. C**51**, 38 (1995).

[2] R. Machleidt, F. Sammarruca, and Y. Song, Phys. Rev. C**53**, R1483 (1996).

[3] V.G.J. Stoks, R.A.M. Klomp, C.P.F. Terheggen, J.J. de Swart, Phys. Rev. C**49**, 2950 (1994).

[4] J.L. Friar et al., Phys. Lett. B**311**, 4 (1993).

[5] A. Nogga, D. Hüber, H. Kamada, and W. Glöckle, Phys. Lett. B**409**, 19 (1997).

[6] H. Witała, W. Glöckle, D. Hüber, J. Golak, and H. Kamada, Phys. Rev. Lett. **81**, 1183 (1998).

[7] K. Sekiguchi et al., Phys. Rev. C**65**, 034003 (2002).

[8] H. Witała et al., Phys. Rev. C**63**, 024007 (2001).

[9] W.P. Abfalterer et al., Phys. Rev. Lett. **81**, 57 (1998).

[10] H. Witała et al., Phys. Rev. C**59**, 3035 (1999).

[11] H. Witała, J. Golak, W. Glöckle, H. Kamada, Phys. Rev. **C71**, 054001 (2005).

[12] H. Witała, J. Golak, R. Skibiński, W. Glöckle, W.N. Polyzou, H. Kamada, Phys. Rev. **C77**, 034004 (2008).

[13] H. Kamada, W. Glöckle, Phys. Lett. **B 655**, 119 (2007).

[14] F. Coester, S.C. Pieper, F.J.D. Serduke, Phys. Rev. C**11**, 1 (1975).

[15] H. Witała, J. Golak, and R. Skibiński, Phys. Lett. **B 634**, 374 (2006).

[16] R. Skibiński, H. Witała, J. Golak, Eur. Phys. J. **A30**, 369 (2006).

[17] K. Sekiguchi et al., Phys. Rev. **C79**, 054008 (2009).

[18] E. P. Wigner, Annals Math. **40**, 149 (1939).

[19] J.K. Lubanski, Physica (Utrecht) **9**, 310 (1942).

[20] B. Bakamjian and L.H. Thomas, Phys. Rev. **92**, 1300 (1953).

[21] B.D. Keister and W.N. Polyzou, Adv. Nucl. Phys. **20**, 225 (1991).

[22] F. Coester, Helv. Phys. Acta **38**, 7 (1965).

[23] H. Witała, T. Cornelius and W. Glöckle, Few-Body Syst. **3**, 123 (1988).

[24] W. Glöckle, H. Witała, D. Hüber, H. Kamada, J. Golak, Phys. Rep. **274**, 107 (1996).

[25] W. Glöckle, T-S.H. Lee, and F. Coester, Phys. Rev. C**33**, 709 (1986).

[26] W. Glöckle, The Quantum Mechanical Few-Body Problem, Springer-Verlag 1983.

[27] D. Hüber, H. Kamada, H. Witała, and W. Glöckle, Acta Physica Polonica **B28**, 1677 (1997).

[28] D. Hüber, H. Witała, and W. Glöckle, Few-Body Syst. **14**, 171 (1993).

[29] J. Golak et al., Phys. Rev. **C 81**, 034006 (2010).

[30] R. Skibiński et al., arXiv: nucl-th 1101.2150.

[31] S.A. Coon et al., Nucl. Phys. **A317**, 242 (1979).

[32] S.A. Coon and W. Glöckle, Phys. Rev. C**23**, 1790 (1981).

[33] S.A. Coon and H.K. Han, Few Body Syst. **30**, 131 (2001).

[34] B.S. Pudliner et al., Phys. Rev. C**56**, 1720 (1997).

[35] K. Sekiguchi et al., Phys. Rev. **C70**, 014001 (2004).

[36] Y. Maeda et al., Phys. Rev. **C76**, 014004 (2007).

[37] K. Hatanaka et al., Phys. Rev. C**66**, 044002 (2002).

[38] J. Kuroś-Żołnierczuk et al., Phys. Rev. **C 66**, 024003 (2002).

[39] E. Epelbaum et al., Phys. Rev. C **66**, 064001 (2002).

[40] B.v. Przevoski et al., Phys. Rev. C**74**, 064003 (2006).

[41] W. Pairsuwan, *et al.* Phys. Rev. **C52**, 2552 (1995).

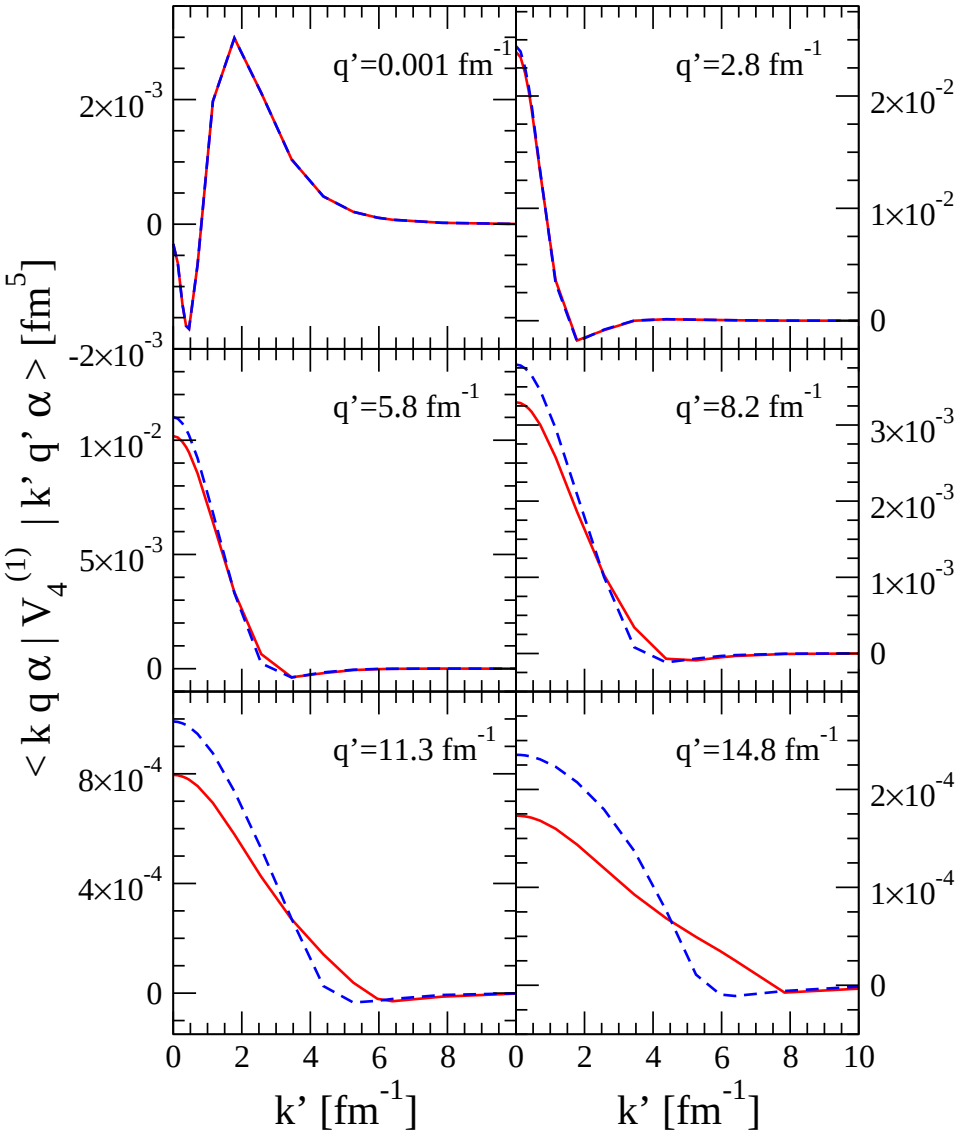

FIG. 1: (color online) The matrix element of the TM99 3NF in relativistic- ($\langle k,q,\alpha|V_4^{(1)}|k',q',\alpha\rangle$ - blue dashed line) and nonrelativistic-basis ($\langle p,q,\alpha|V_4^{(1)}|p',q',\alpha\rangle$ - red solid line) for the total angular momentum and parity of the 3N system $J^\pi = \frac{1}{2}^+$ and channel $\alpha = |(00)0(0\frac{1}{2})\frac{1}{2}(1\frac{1}{2})\frac{1}{2}>$. The momenta $p = k = 0.132$ fm^{-1} and $q = 0.132$ fm^{-1}.

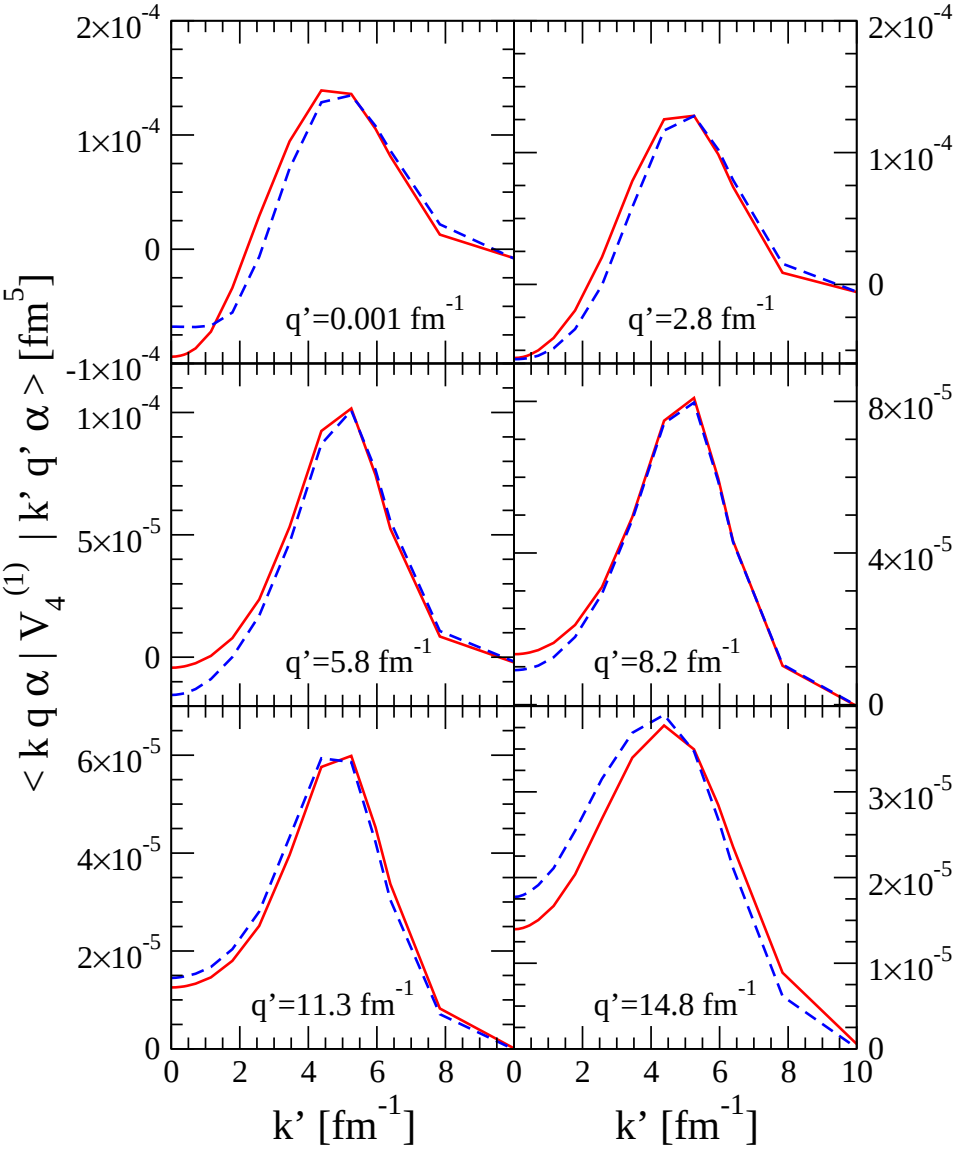

FIG. 2: (color online) The same as in Fig. 1 but for the momenta $p = k = 5.25$ fm^{-1} and $q = 8.24$ fm^{-1}.

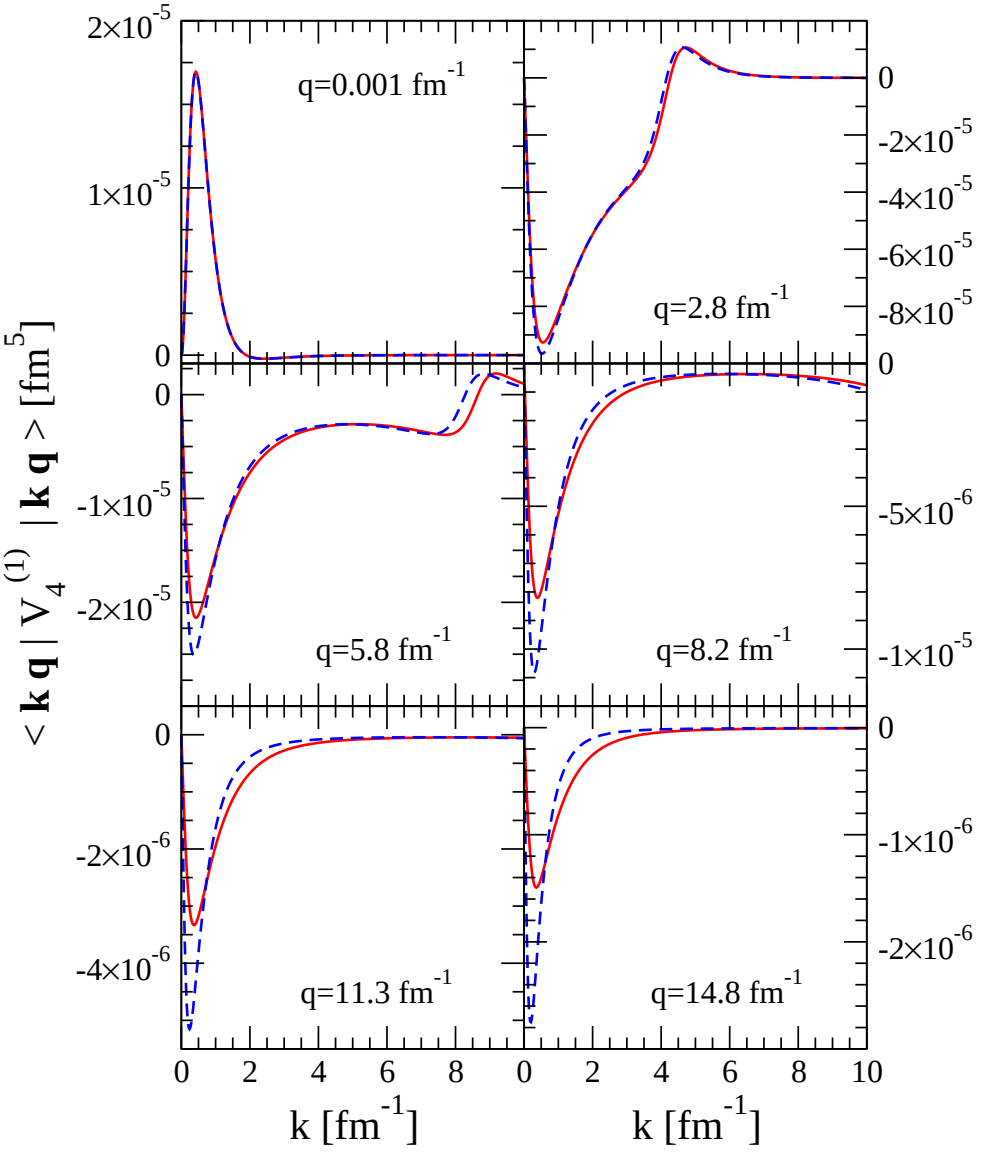

FIG. 3: (color online) The matrix element of the TM99 3NF in relativistic- ($\langle \mathbf{k},\mathbf{q}|V_4^{(1)}|\mathbf{k},\mathbf{q}\rangle$ - blue dashed line) and nonrelativistic-basis ($\langle \mathbf{p},\mathbf{q}|V_4^{(1)}|\mathbf{p},\mathbf{q}\rangle$ - red solid line). They are shown as a function of k at a number of q values assuming that all momenta are parallel to the unit vector $\left(\frac{1}{\sqrt{3}},\frac{1}{\sqrt{3}},\frac{1}{\sqrt{3}}\right)$, all spin magnetic quantum numbers in the initial and final state are equal $\frac{1}{2}$, and isospins $t=t'=0$.

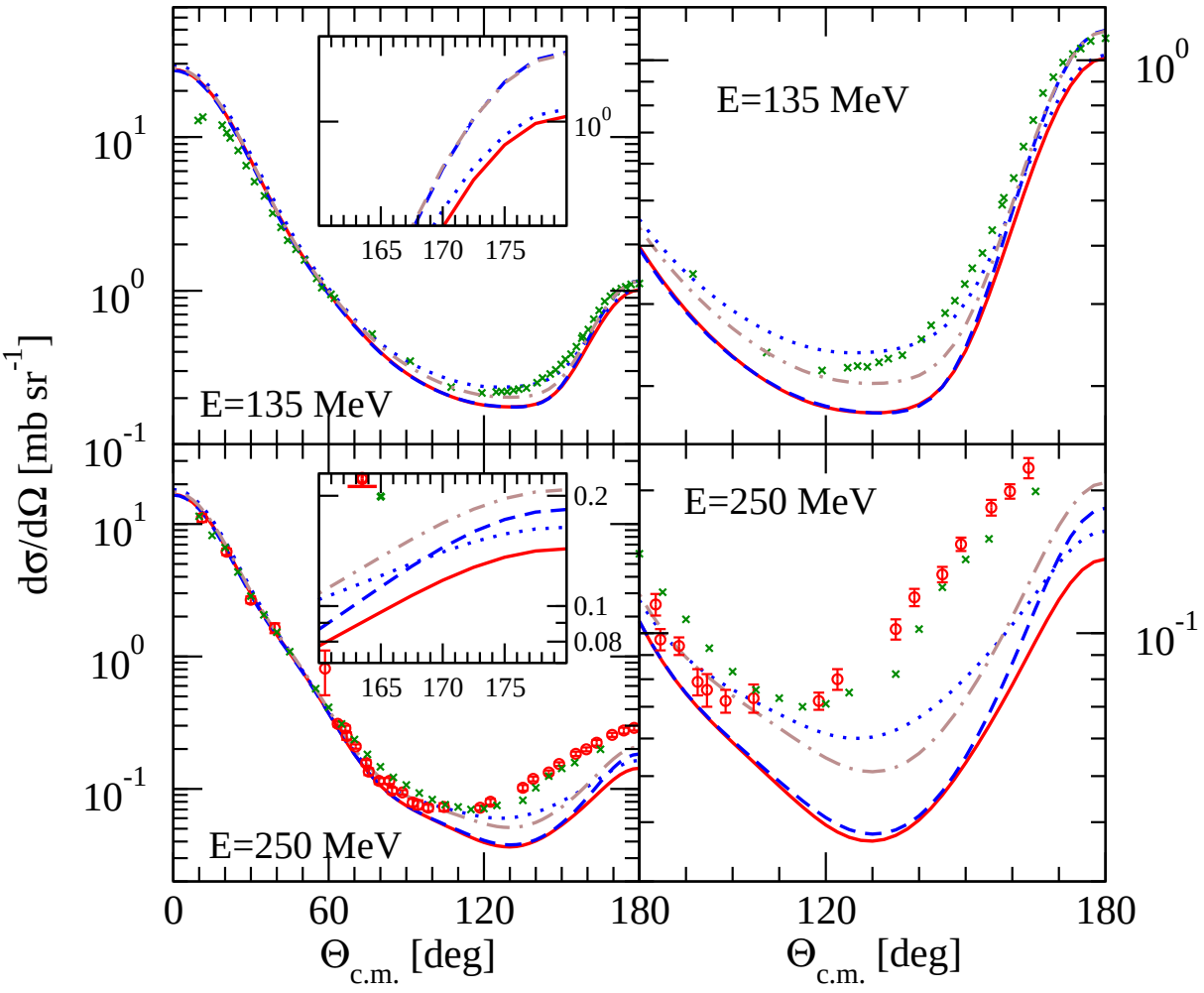

FIG. 4: (color online) The elastic nd scattering angular distributions at the incoming neutron lab. energy E = 135 and 250 MeV. The solid (red) and dotted (blue) lines are results of the non-relativistic Faddeev calculations with the CD Bonn potential alone and combined with TM99 three-nucleon force, respectively. The relativistic predictions based on CD Bonn potential without Wigner spin rotations are shown by the dashed (blue) lines. The dashed-dotted (brown) lines show results of relativistic calculations with the TM99 three-nucleon force included. The pd data (x-es) at 135 MeV are from ref. [7] and at 250 MeV from ref. [37]. At 250 MeV also nd data of ref. [36] are shown by circles. The inserts and figures in the right column display details of the cross sections in specific angular ranges.

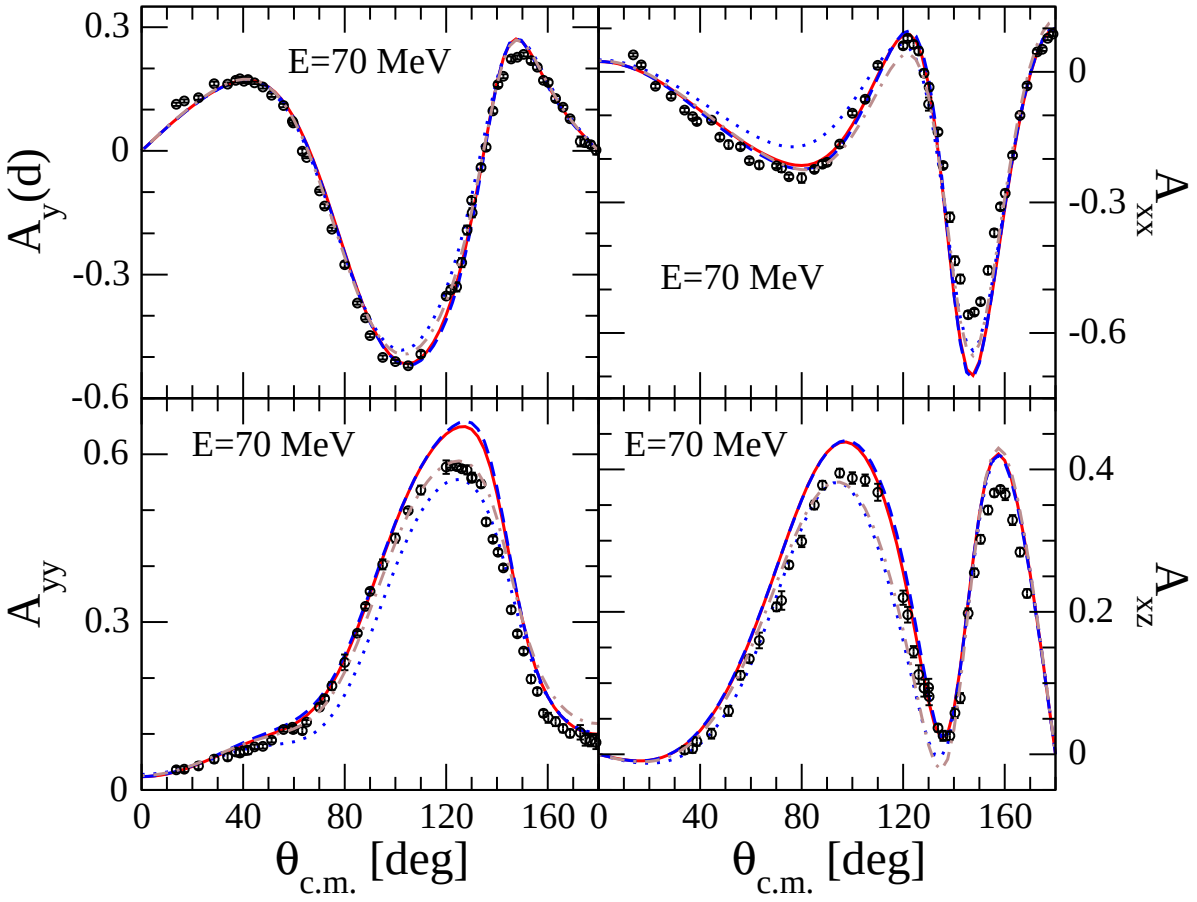

FIG. 5: (color online) The vector (deuteron) $A_y(d)$ and tensor analyzing powers A_{xx}, A_{yy}, and A_{xz} in elastic nd scattering at the incoming neutron lab. energy $E = 70$ MeV. For description of lines see Fig.4. The pd data (open circles) are from [7].

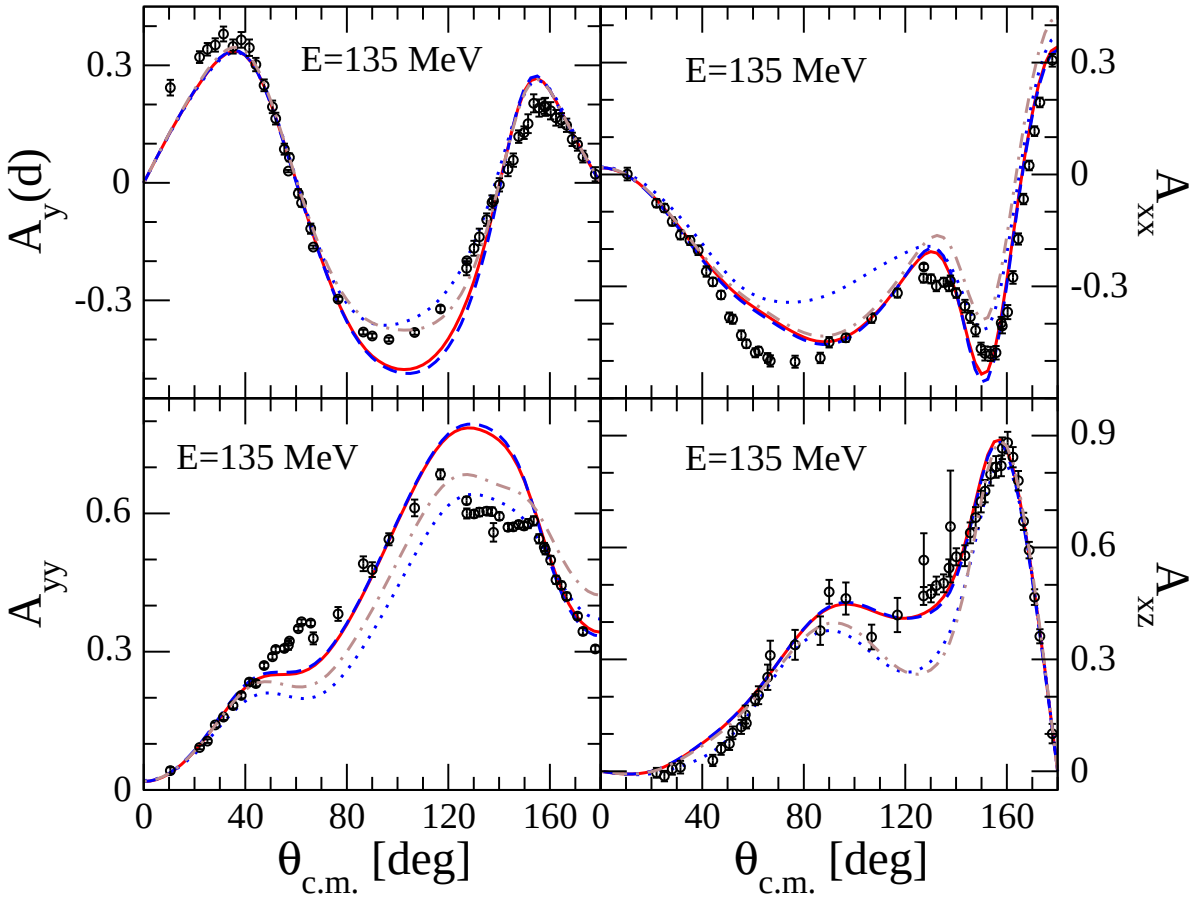

FIG. 6: (color online) The vector (deuteron) $A_y(d)$ and tensor analyzing powers A_{xx}, A_{yy}, and A_{xz} in elastic nd scattering at the incoming neutron lab. energy $E = 135$ MeV. For description of lines see Fig.4. The pd data (open circles) are from [7].

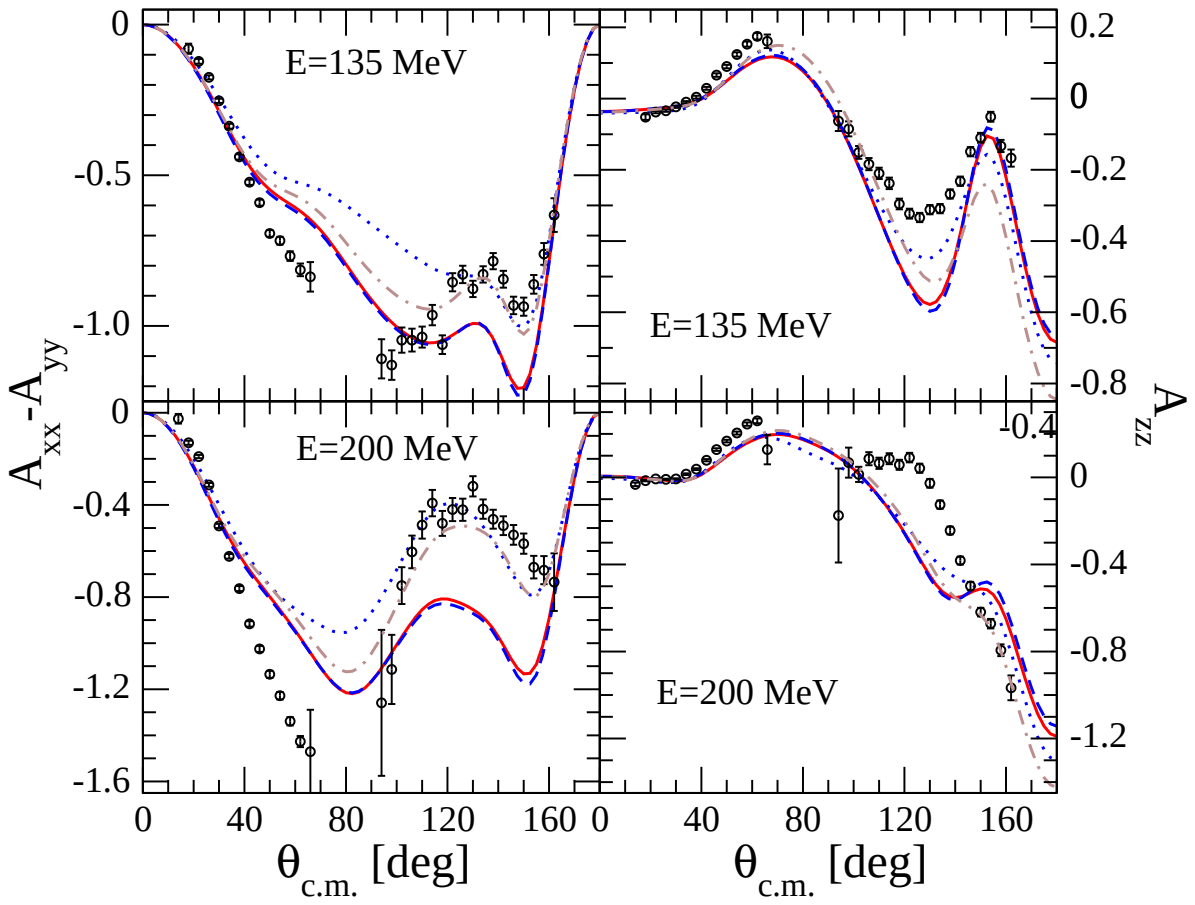

FIG. 7: (color online) The tensor analyzing powers $A_{xx} - A_{yy}$ and A_{zz} in elastic nd scattering at the incoming neutron lab. energy $E = 135$ and $E = 200$ MeV. For description of lines see Fig.4. The pd data (open circles) are from [40].

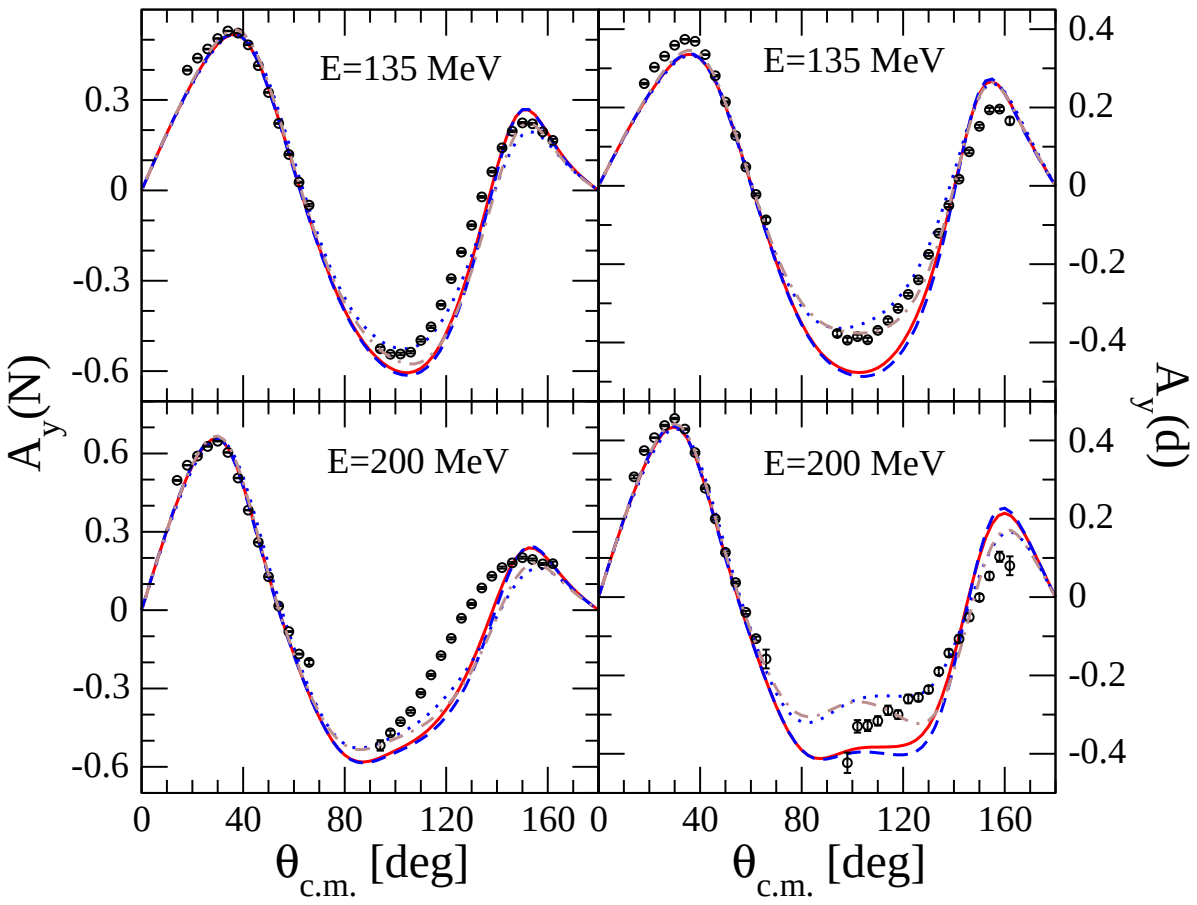

FIG. 8: (color online) The vector analyzing powers $A_y(N)$ and $A_y(d)$ in elastic nd scattering at the incoming neutron lab. energy $E = 135$ and $E = 200$ MeV. For description of lines see Fig.4. The pd data (open circles) are from [40].

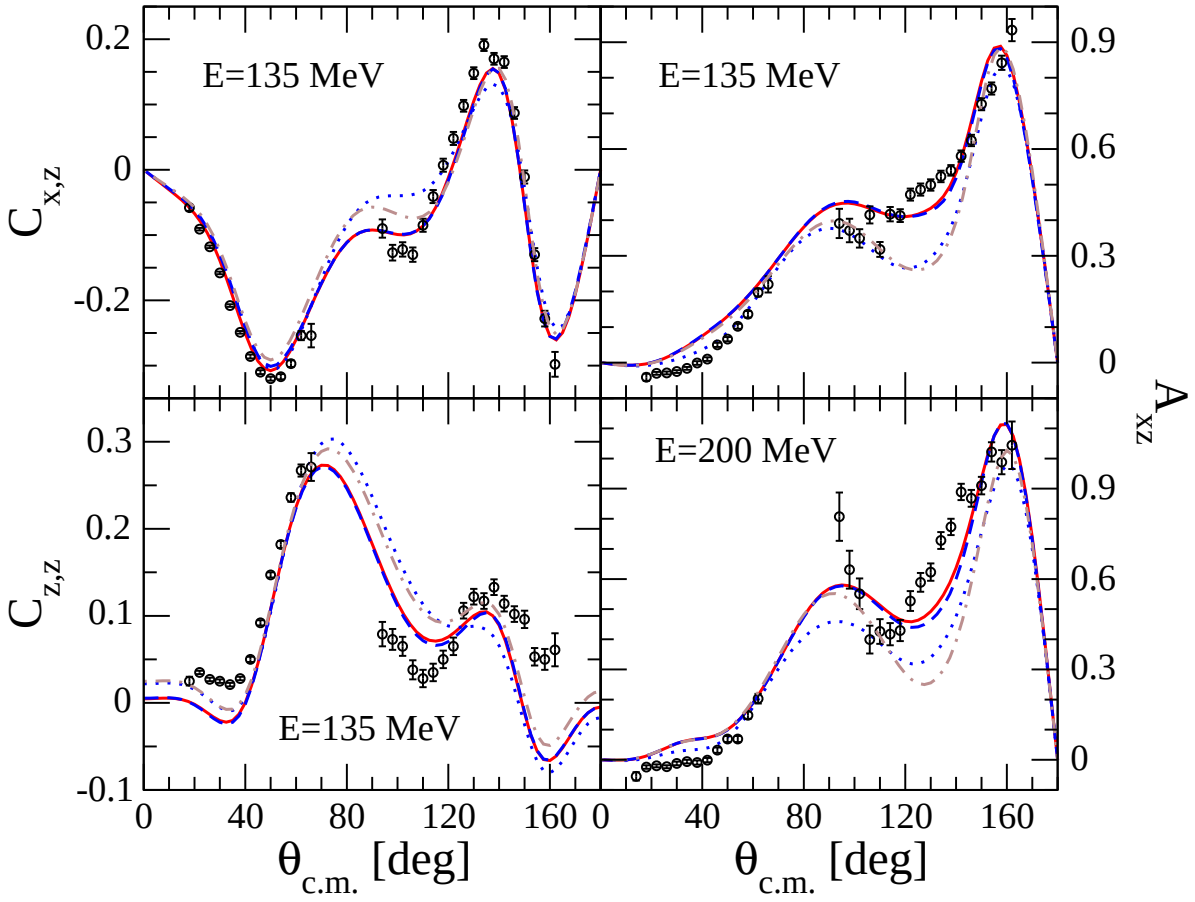

FIG. 9: (color online) The spin correlation coefficients $C_{x,z}$ and $C_{z,z}$ and tensor analyzing power A_{xz} in elastic nd scattering at the incoming neutron lab. energy $E = 135$ and 200 MeV. For description of lines see Fig.4. The pd data (open circles) are from [40].

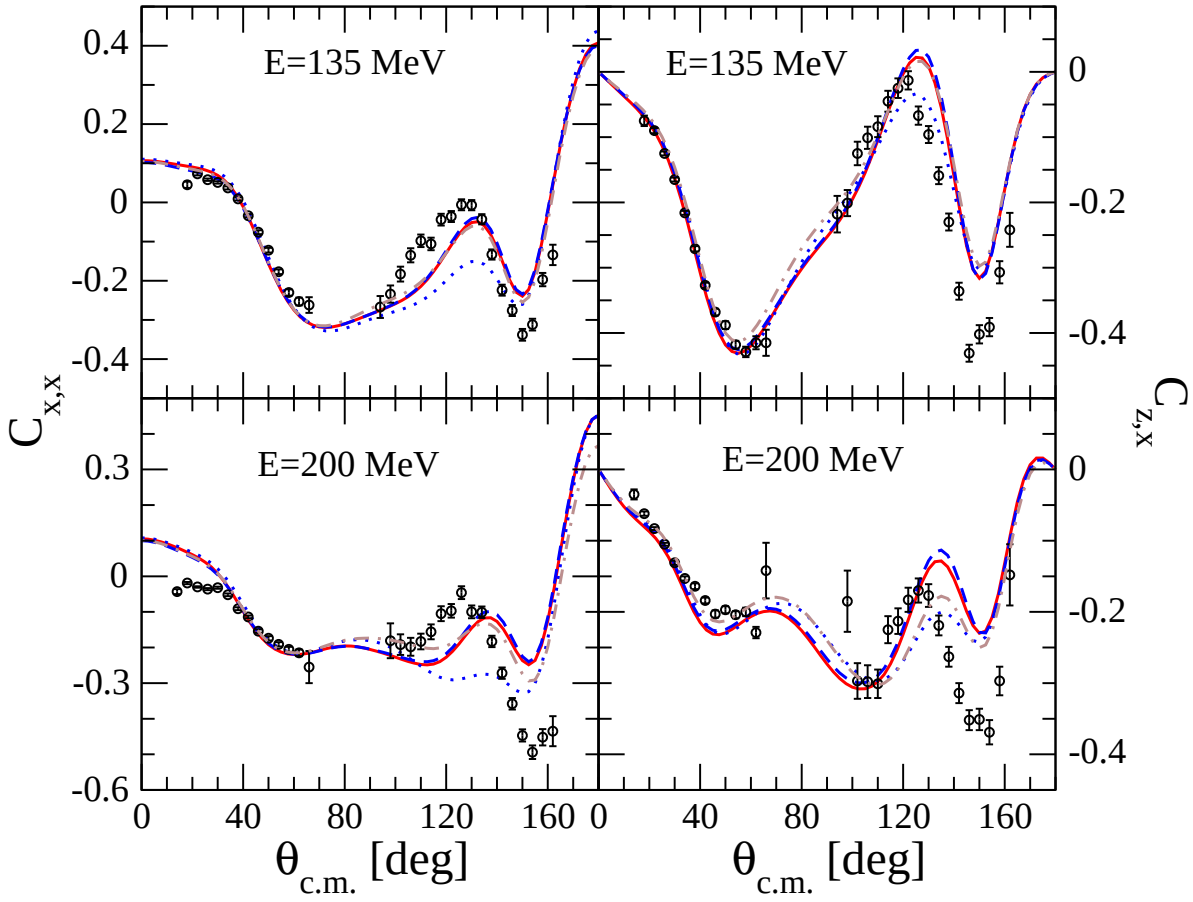

FIG. 10: (color online) The spin correlation coefficients $C_{x,x}$ and $C_{z,x}$ in elastic nd scattering at the incoming neutron lab. energy $E = 135$ and 200 MeV. For description of lines see Fig.4. The pd data (open circles) are from [40].

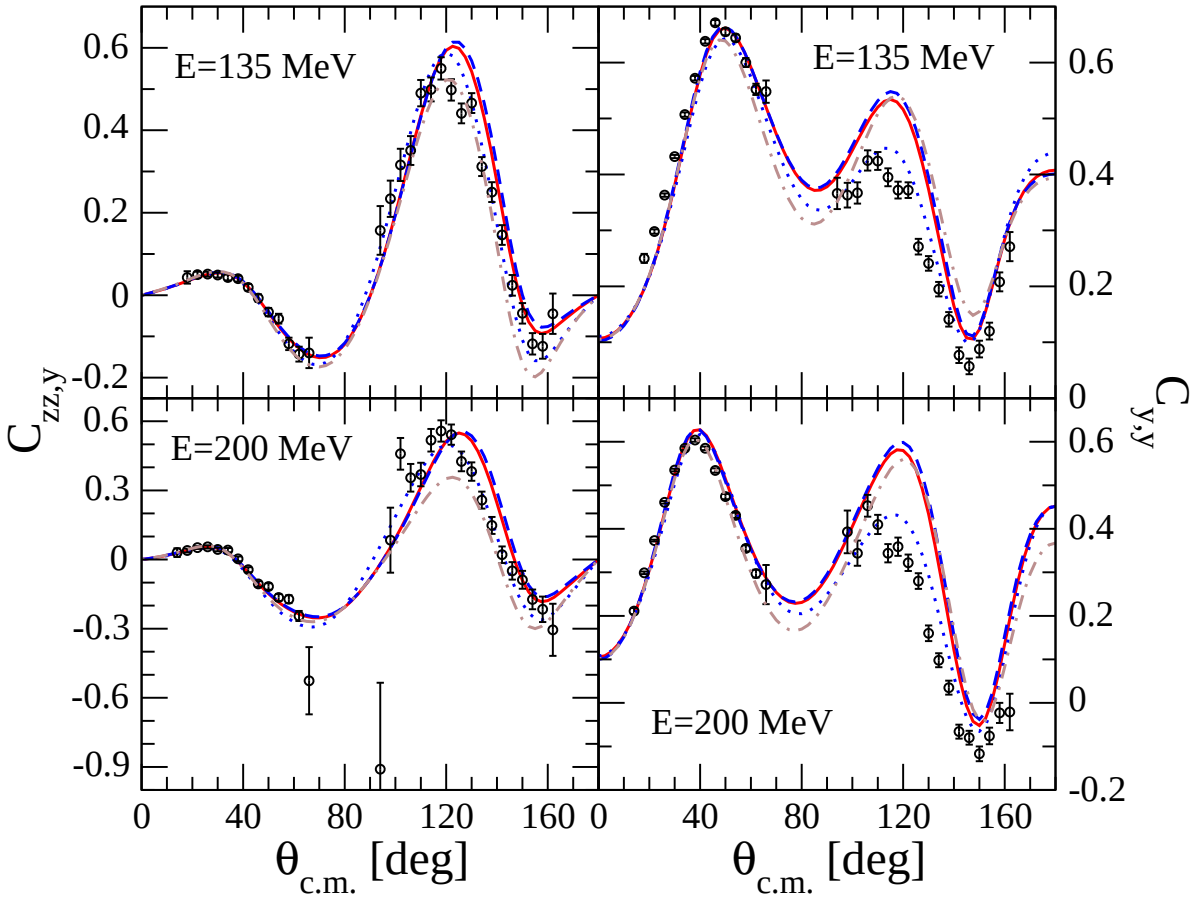

FIG. 11: (color online) The spin correlation coefficients $C_{zz,y}$ and $C_{y,y}$ in elastic nd scattering at the incoming neutron lab. energy $E = 135$ and 200 MeV. For description of lines see Fig.4. The pd data (open circles) are from [40].

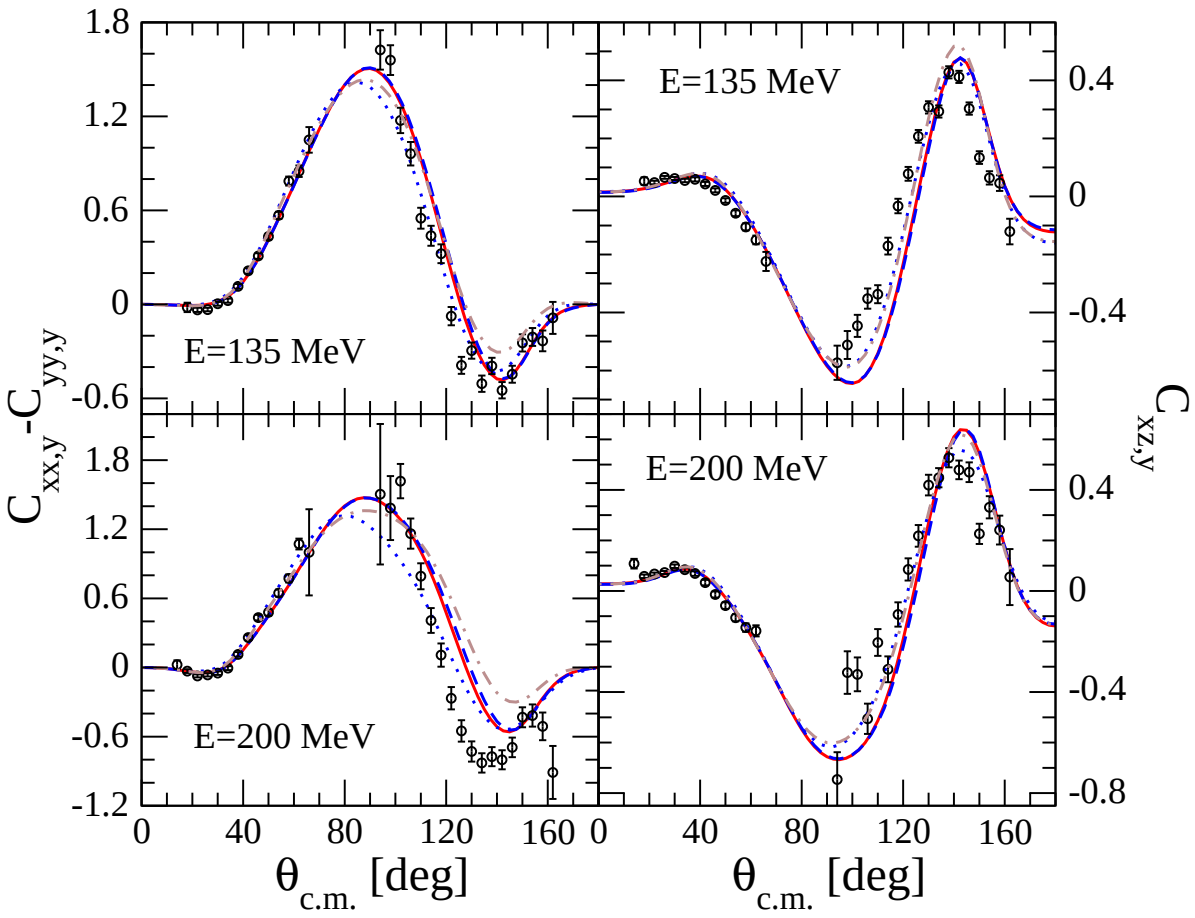

FIG. 12: (color online) The spin correlation coefficients $C_{xx,y} - C_{yy,y}$ and $C_{xz,y}$ in elastic nd scattering at the incoming neutron lab. energy $E = 135$ and 200 MeV. For description of lines see Fig.4. The pd data (open circles) are from [40].

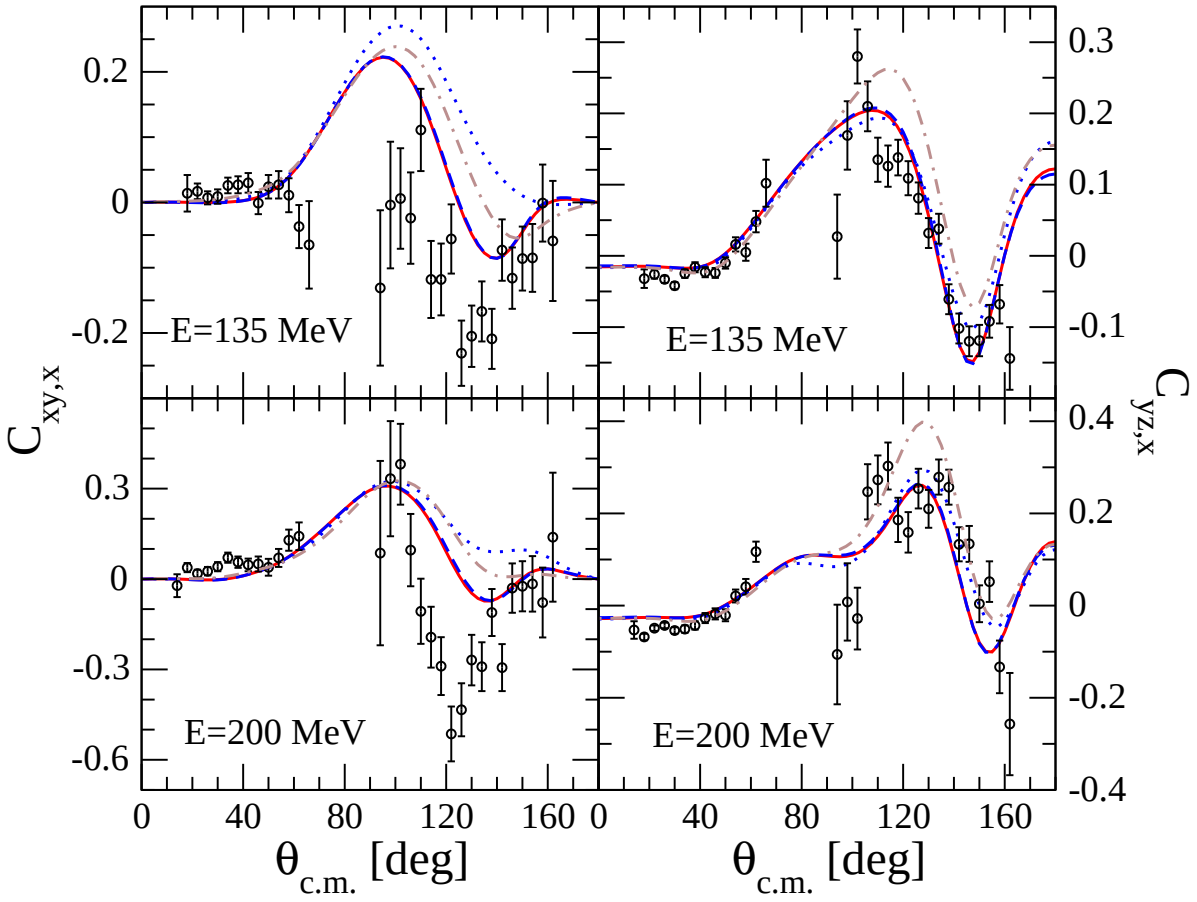

FIG. 13: (color online) The spin correlation coefficients $C_{xy,x}$ and $C_{yz,x}$ in elastic nd scattering at the incoming neutron lab. energy $E = 135$ and 200 MeV. For description of lines see Fig.4. The pd data (open circles) are from [40].

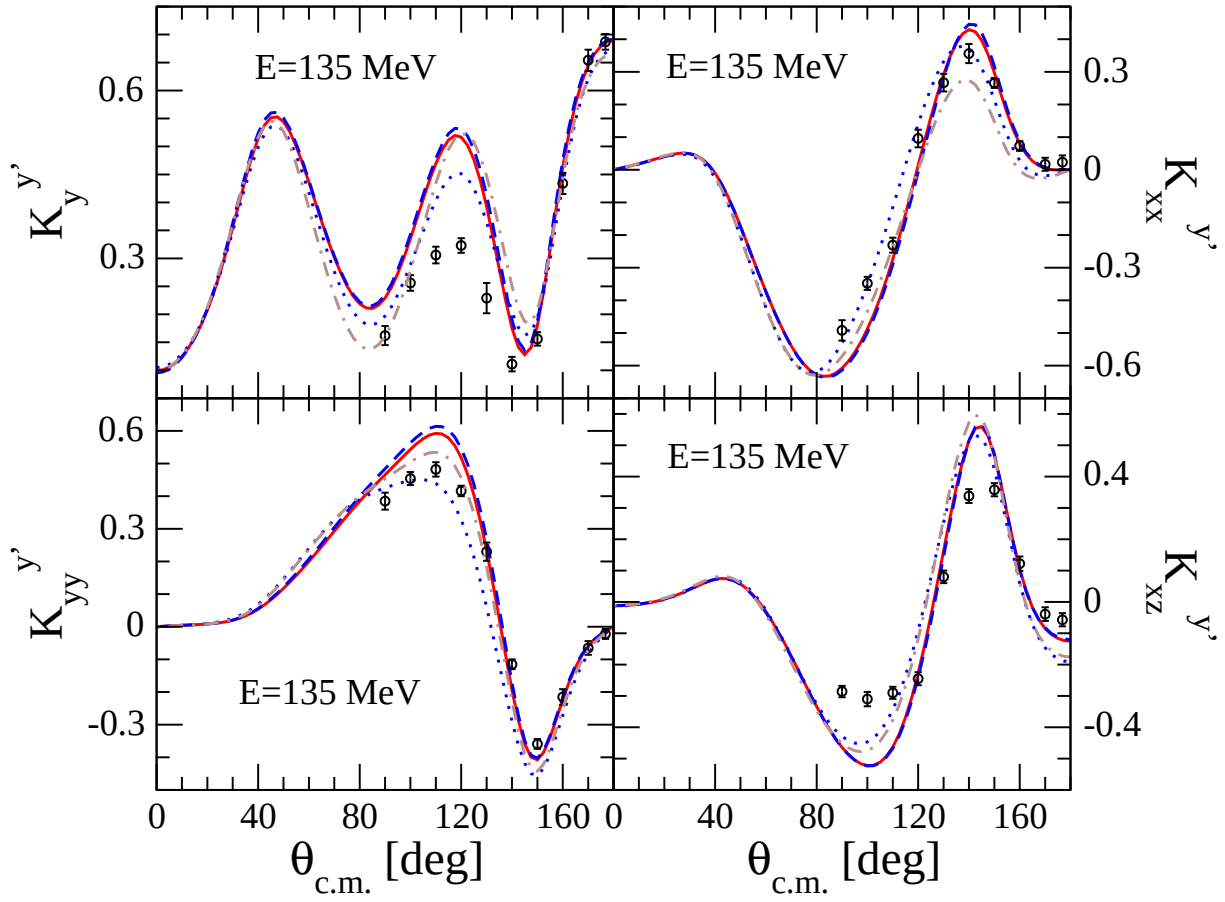

FIG. 14: (color online) The deuteron to neutron polarization transfer coefficients $K_y^{y'}$, $K_{xx}^{y'}$, $K_{yy}^{y'}$, and $K_{xz}^{y'}$ in elastic nd scattering at the incoming neutron lab. energy $E = 135$ MeV. For description of lines see Fig.4. The pd data (open circles) are from [35].

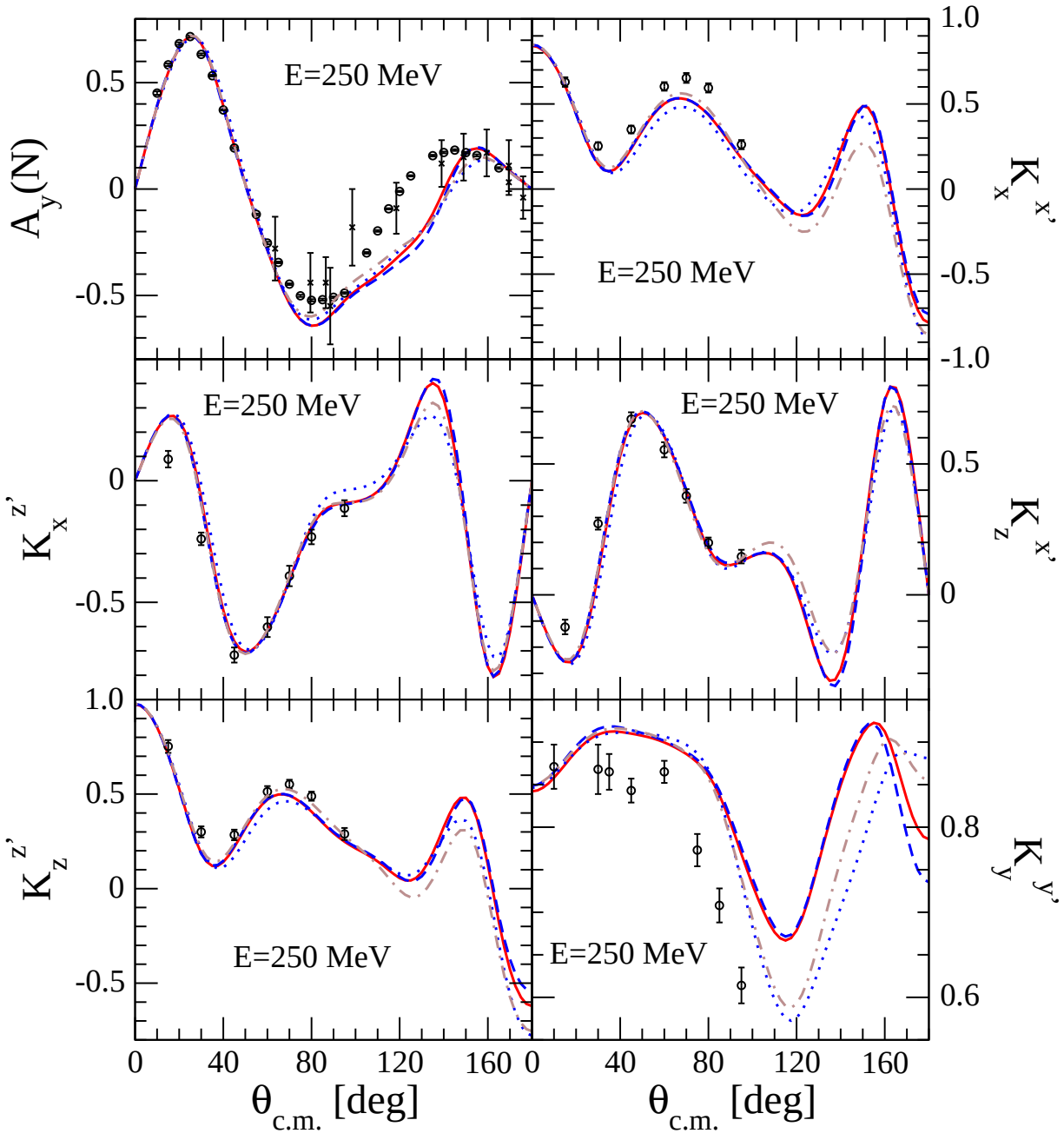

FIG. 15: (color online) The neutron analyzing power $A_y(N)$ and neutron to neutron polarization transfer coefficients $K_x^{x'}$, $K_x^{z'}$, $K_z^{x'}$, $K_z^{z'}$, and $K_y^{y'}$ in elastic nd scattering at the incoming neutron lab. energy $E = 250$ MeV. For description of lines see Fig.4. The pd data (open circles) are from [37]. The nd data for $A_y(N)$ (x-es) are from [36]

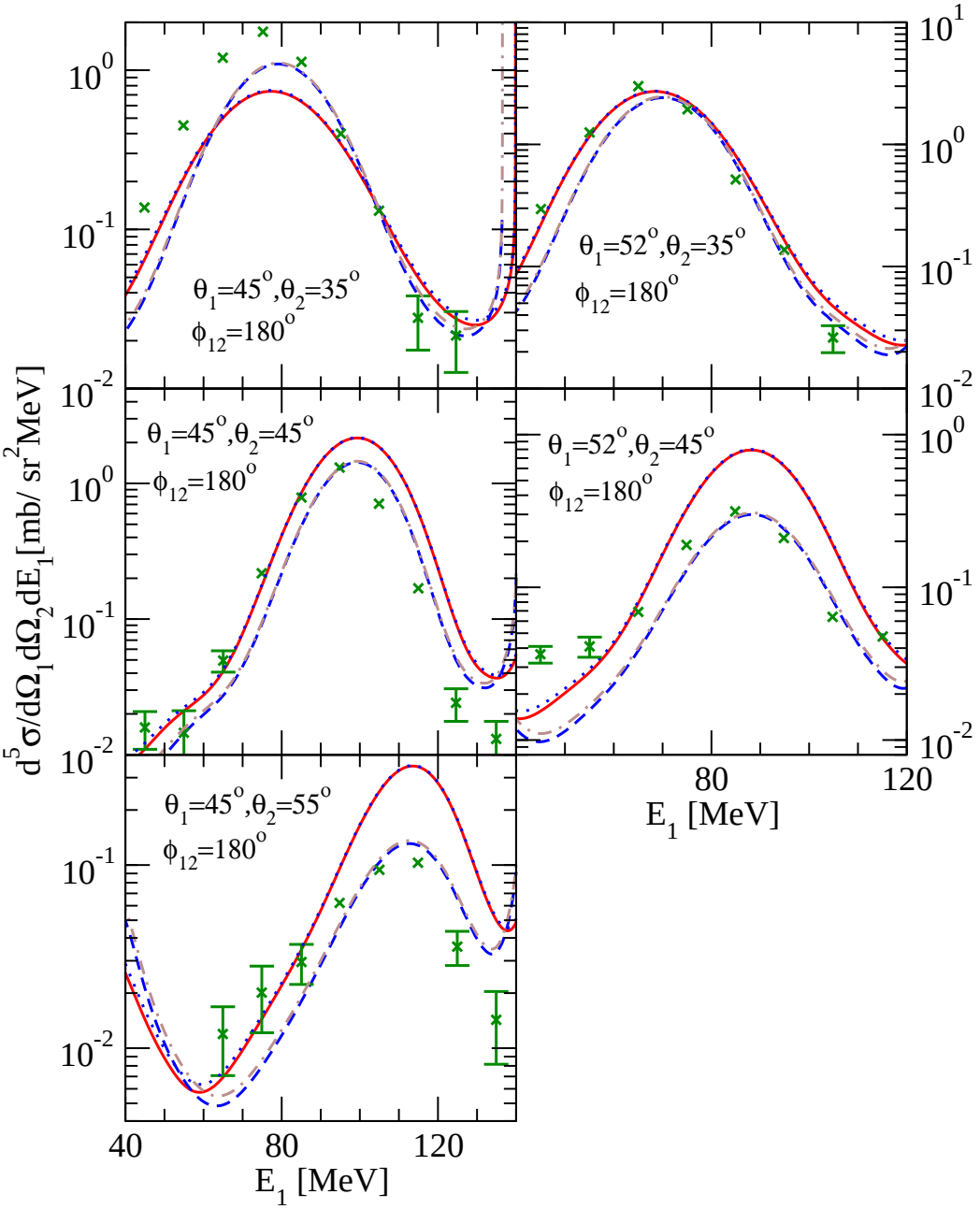

FIG. 16: (color online) The five-fold cross section $d^5\sigma/d\Omega_1 d\Omega_2 dE_1^{lab}$ for the breakup reaction d(n,np)n at $E_n^{lab} = 200$ MeV and fixed angles of outgoing nucleons 1 and 2 as indicated in the figures. For description of lines see Fig.4. The d(p,pn)p data (x-es) are from [41].

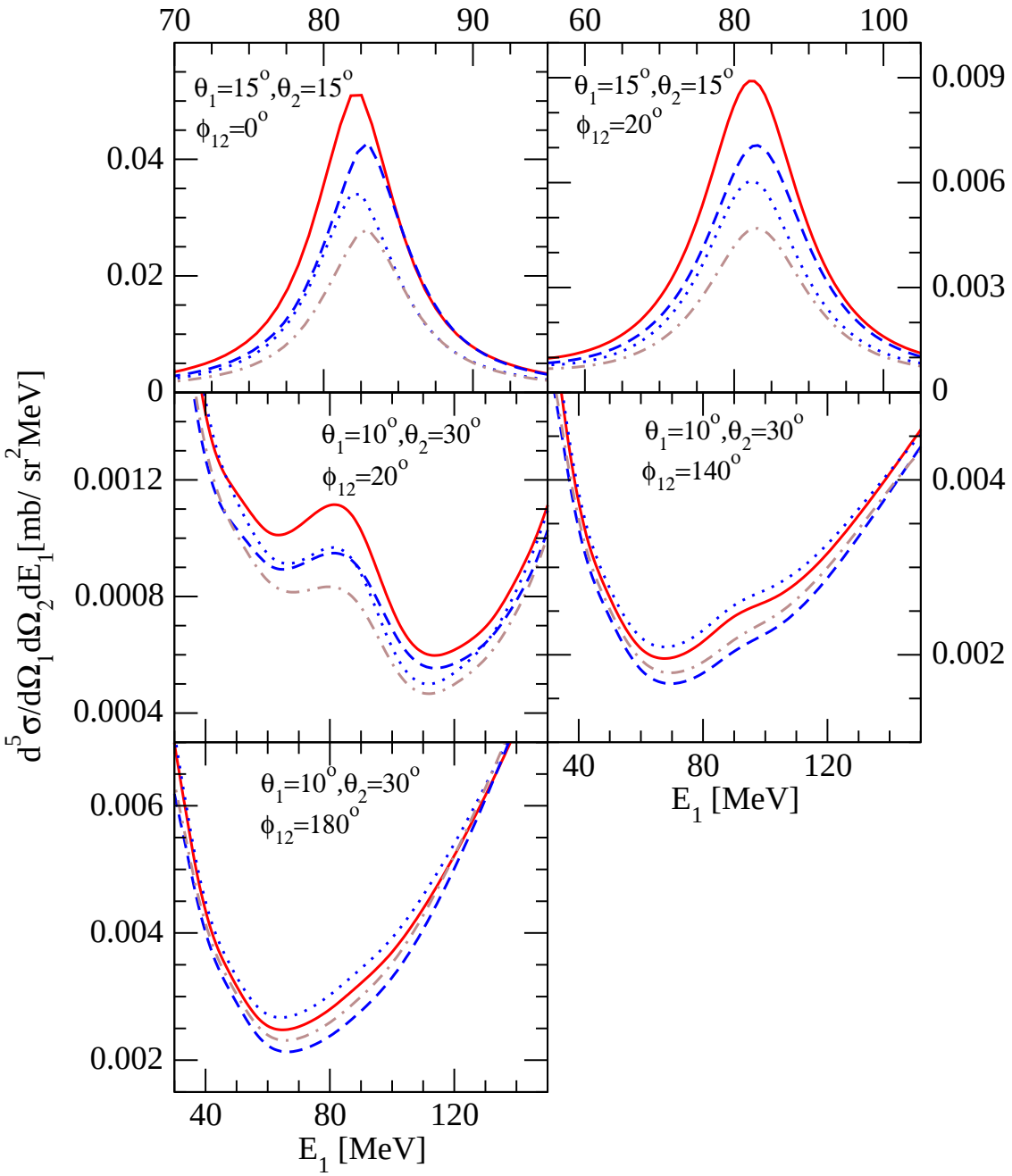

FIG. 17: (color online) The five-fold cross section $d^5\sigma/d\Omega_1 d\Omega_2 dE_1^{lab}$ for the breakup reaction d(n,np)n at $E_n^{lab} = 200$ MeV and fixed angles of outgoing nucleons 1 and 2 as indicated in the figures. For description of lines see Fig.4.

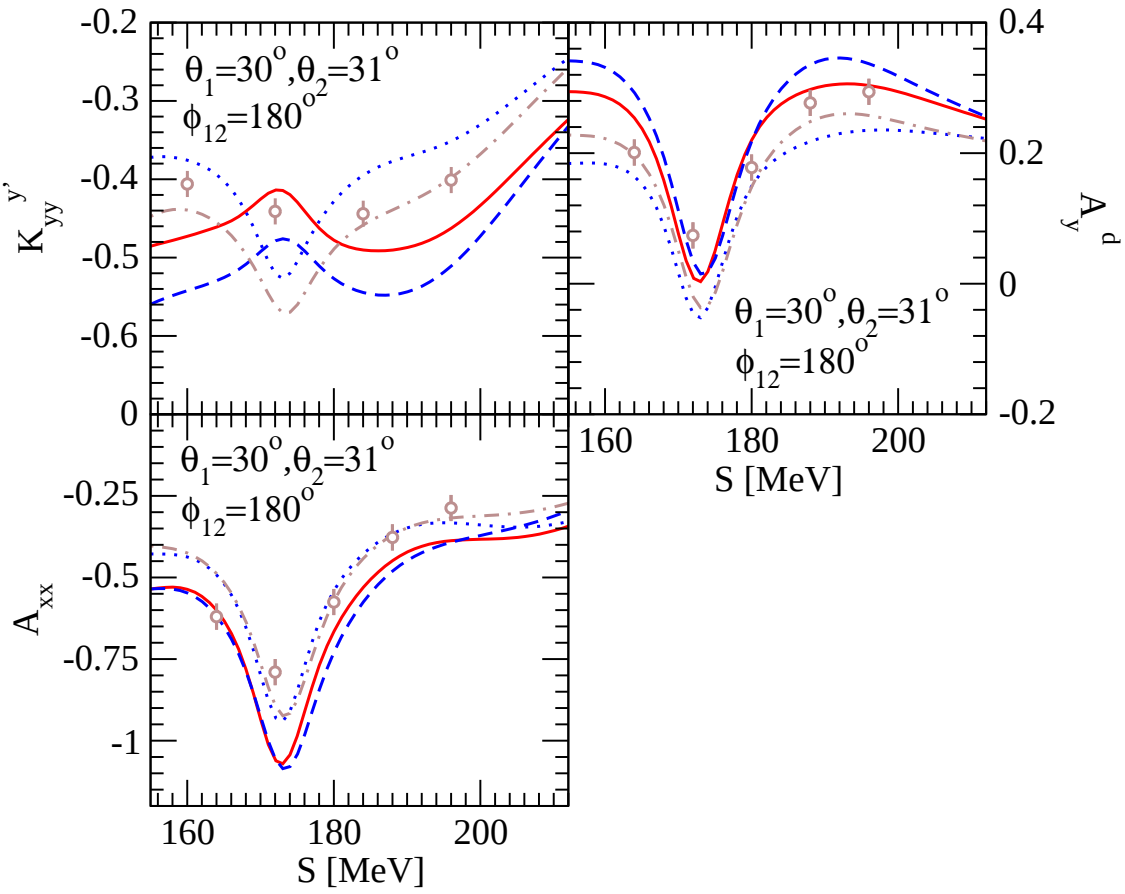

FIG. 18: (color online) The polarization transfer coefficient $K_{yy}^{y'}$ and deuteron analyzing powers A_y^d and A_{xx} in the breakup reaction n(d,nn)p at incoming deuteron lab. energy $E_d^{lab} = 270$ MeV, shown as a function of the S-curve arc length. For description of lines see Fig.4. The 270 MeV dp data (circles) are from ref. [17].